Science of the Total Environment 895 (2023) 164908

Contents lists available at ScienceDirect

Science of the Total Environment

journal homepage: www.elsevier.com/locate/scitotenv

Hotspots of microplastic accumulation at the land-sea transition and their spatial heterogeneity: The Po River prodelta (Adriatic Sea)

C. Pellegrini [a,*], F. Saliu [b], A. Bosman [c], I. Sammartino [a], C. Raguso [b], A. Mercorella [a], D.S. Galvez [a], A. Petrizzo [a], F. Madricardo [a], M. Lasagni [b], M. Clemenza [d], F. Trincardi [e], M. Rovere [a]

[a] Consiglio Nazionale delle Ricerche (CNR), Istituto di Scienze Marine (ISMAR-CNR), Italy
[b] Earth and Environmental Science Department, University of Milano Bicocca, Milano, Italy
[c] Consiglio Nazionale delle Ricerche (CNR), Istituto di Geologia Ambientale e Geoingegneria (IGAG), Italy
[d] INFN Sezione di Milano-Bicocca, Piazza della Scienza 3, 20126 Milano, Italy
[e] Consiglio Nazionale delle Ricerche (CNR), Dipartimento di Scienze del Sistema Terra e Tecnologie per l'Ambiente (DSSTTA), Rome, Italy

HIGHLIGHTS

- River prodelta are pools of Microplastics (MPs), Phthalates, and cellulosic fibers
- MP abundances were investigated based on morpho-bathymetry and flood occurrence
- Lateral heterogeneity of MPs and cellulose fibers in Po River Podelta sediments are related to depositional processes
- Sites contaminated by MPs are distal reaches of delta lobe and migrating bedforms with maximum concentration of 625 MPs/kg
- A large abundance of cellulose fibers was found

GRAPHICAL ABSTRACT

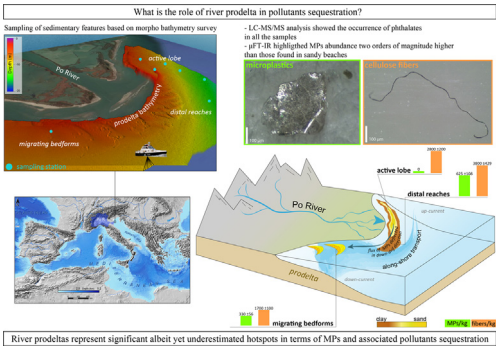

ARTICLE INFO

Editor: Damià Barceló

Keywords:
Microplastics
Phthalates
Impact on marine food-chain
River delta
Sedimentary processes
Hot spots

ABSTRACT

Deltas are the locus of river-borne sediment accumulation, however, their role in sequestering plastic pollutants is still overlooked. By combining geomorphological, sedimentological, and geochemical analyses, which include time-lapse multibeam bathymetry, sediment provenance, and µFT-IR analyses, we investigate the fate of plastic particles after a river flood event providing an unprecedented documentation of the spatial distribution of sediment as well as of microplastics (MPs), including particles fibers, and phthalates (PAEs) abundances in the subaqueous delta. Overall sediments are characterized by an average of 139.7 ± 80 MPs/kg d.w., but display spatial heterogeneity of sediment and MPs accumulation: MPs are absent within the active sandy delta lobe, reflecting dilution by clastic sediment (ca. 1.3 Mm^3) and sediment bypass. The highest MP concentration (625 MPs/kg d.w.) occurs in the distal reaches of the active lobe where flow energy dissipates. In addition to MPs, cellulosic fibers are relevant (of up to 3800 fibers/kg d.w.) in all the analyzed sediment samples, and dominate (94 %) with respect to synthetic polymers.
Statistically significant differences in the relative concentration of fiber fragments ≤0.5 mm in size were highlighted between the active delta lobe and the migrating bedforms in the prodelta. Fibers were found to slightly follow a power law size distribution coherent with a one-dimensional fragmentation model and thus indicating the absence of a size dependent selection mechanism during burial. Multivariate statistical analysis suggests traveling distance and bottom-transport regime as the most relevant factors controlling particle distribution. Our findings suggest that subaqueous prodelta should be considered hot spots for the accumulation of MPs and associated pollutants, albeit the strong lateral heterogeneity in their abundances reflects changes in the relative influence of fluvial and marine processes.

* Corresponding author.
E-mail address: claudio.pellegrini@bo.ismar.cnr.it (C. Pellegrini).

http://dx.doi.org/10.1016/j.scitotenv.2023.164908
Received 27 March 2023; Received in revised form 7 June 2023; Accepted 13 June 2023
Available online 27 June 2023

1. Introduction

Plastic pollution greatly affects the marine environment (Thompson et al., 2009a, 2009b) and extends from the sea surface to the deepest seafloor, the ultimate sink for plastic debris (Woodall et al., 2014, Galgani, 2015, Lebreton et al., 2019; Martin et al., 2022; Canals et al., 2021; Garcés-Ordóñez et al., 2022). Coastal systems are the main temporary sink for river-borne sediments (e.g. Bianchi et al., 2018; Pellegrini et al., 2021), and have the potential of sequestering anthropogenic material derived from the catchments (Simon-Sánchez et al., 2019; Trincardi et al., 2023). However, the role of deltas in sequestering MPs is still poorly studied, hindering our ability to derive a global picture of MPs distribution at the land-ocean interface (Weiss et al., 2021) and improve mitigation measures. Among coastal systems, river deltas are highly dynamic environments and respond quickly to natural and human changes (Orton and Reading, 1993; Blum and Roberts, 2009; Syvitski et al., 2009; Maselli and Trincardi, 2013; Dai et al., 2014; Bosman et al., 2020; Trincardi et al., 2020, 2023), and are exposed to strong human pressures (Overeem and Brakenridge, 2009) which alter river flow, sediment discharge, and coastline dynamics (Syvitski et al., 2005a, 2005b; Hood, 2010; Anthony et al., 2014; IPCC, 2021; Pellegrini et al., 2021; Trincardi et al., 2023).

A revision of the current literature reveals that the contribution of rivers to global plastic pollution is still debated (Lebreton et al., 2017; Schmidt et al., 2017; Hurley et al., 2018; Kane et al., 2020; Pierdomenico et al., 2022; Waldschläger et al., 2022; Kelleher et al., 2023; Kurki-Fox et al., 2023). Recent studies such as those from the Ebro River (Simon-Sánchez et al., 2019), Yellow River (Duan et al., 2020), Yangtze River (Hu et al., 2018), Ganga River (Singh et al., 2021), Po River (Piehl et al., 2019), Nile River (Shabaka et al., 2022), and Mekong River (Nguyen et al., 2022) highlighted how sediments in wetlands are important sinks for MP pollutants and how hydrological flow and sediment transport dynamics might facilitate the deposition of MPs in seafloor sediments. However, the concentration of plastic pollution in these transitional environments remains poorly constrained (Leslie et al., 2017), especially in prodeltas that are the delta sector lying beyond the delta front in a submerged environment and that records high sediment accumulation rate (Coleman and Wright, 1975; Pellegrini et al., 2020). Prodelta depositional systems act as direct sinks for vast quantities of terrigenous sediment, organic carbon, and anthropogenic pollutants, and represent valuable archives of environmental change increasing human pressure on it (e.g. Syvitski et al., 2022). In these systems, our understanding of the distribution of pollutant particles and the preservation of environmental signals is hampered by the limited ability to access the shallow and energetic subaqueous realm.

By questioning if prodeltas are main sector of MPs accumulation as well, we provide the first evaluation of MPs and phthalates in the prodelta of the Po River (North Adriatic Sea), a large delta with an anthropogenically modified catchment of 68.800 km^2, as well as one of the largest deltaic systems of the Mediterranean region, a region characterized by high accumulation of plastic debris (Cózar et al., 2014; Suaria et al., 2016; Duncan et al., 2018; Pierdomenico et al., 2022; Boucher and Bilard, 2020; Baudena et al., 2022).

Here, we document the occurrence of MPs, fibers and phthalates in the Po Delta throughout sediment samples representative of the sedimentary features present at the seafloor and selected based on morphodynamic survey defining: 1) concentration and fluxes of MPs offshore the Po di Pila mouth, the most active branch of the Po River; 2) particle characteristics (type of polymer, size, color), and their spatial distribution, after a major river-flood event. Our overarching goal is to: i) identify any possible correlation between sediment and plastic particle accumulation, in particular investigate the relationship between MPs and phthalates and delta subenvironments defined by geomorphological descriptors; ii) describe relationship between sediment distribution and plastic-contaminants concentrations at the scale of mobile bedforms; iii) determine the relevance of polymer density and particle shape in the MPs transport behavior; and iv) highlight any possible plastic particle partition/selection processes during transport and deposition. Studying the Po prodelta, we attempt a description of the processes leading river prodelta to act as sink for MPs pollutants, and of their contribution to the global inventories of MPs sequestered in temporary storages along the river to sea continuum.

2. Material and methods

2.1. Study area: the Po River Delta

The Po River Delta (Fig. 1a, and b) is one of the largest Mediterranean deltas and a World Heritage Site and Biosphere reserve by UNESCO (Gissi et al., 2014). The Po Delta is a unique habitat supporting immense biodiversity, including over 370 species of birds, mollusks, fish and amphibians. The Po River Delta also represents a tourist destination and a hotspot of fishing (commercial and recreational) and extensive aquaculture (mainly mussels, clams and shrimps), which are the main economic drivers of the area. The Po River Delta is subjected to plastic pollution mainly derived from the Po River catchment, a drainage area of 68.800 km^2 from the western Alps to the Po Alluvial Plain hosting >20 million inhabitants, including major cities and large industrial and agricultural sites.

According to Syvitski et al. (2005b), 61 % of the total freshwater transport and 74 % of sediment load to the delta reaches Po della Pila (Nelson, 1970; Syvitski et al., 2005b; Falcieri et al., 2014), where this study concentrates. The subaqueous geomorphology of the Po della Pila prodelta is strongly influenced by river floods, wind-driven waves, currents and a cyclonic circulation with a marked southward component in the prodelta area (Artegiani et al., 1997; Boldrin et al., 2005; Maicu et al., 2018), coupled with the southbound West Adriatic Coastal Current (Sherwood et al., 2004; Bosman et al., 2020; Trincardi et al., 2020). All these depositional and oceanographic controlling factors together govern the marine plastic discharge in the area (Liubartseva et al., 2016).

The last major river flood occurred in 2019 and lasted for 20 days (2019-11-18 to 2019-12-05) with a daily average discharge reaching 8000 m^3/s with an increase in the hydrometric level up to 5 m (Cavanella gauging station, Fig. 2). Nausicaa buoy (Fig. 2) documented significant wave height < 1.5 m, suggesting reduced energetic conditions during flood deposition. The flooding also recorded the highest plastic water mass in December (5.89 mg m^{-3}) and November (4.58 ± 0.48 mg m^{-3}), with a total 145 tons/year of plastics transported by the river in 2019 (Munari et al., 2021).

2.2. Grab samplings and multibeam bathymetry

The multibeam swath bathymetry and sediment samples were collected in Spring 2021 onboard the R/V Litus during the Picnic survey after the 2019 Po River flood event (see Table 1 for more details), in the same area where previous survey was conducted in the 2016 (Bosman et al., 2020). Multibeam swath bathymetry was collected with a Kongsberg EM 2040C dual-head multi-frequency system pole-mounted on the vessel, used in equidistant mode with a frequency set to 300 kHz with 800 beams (400 per swath). The positioning was carried out using a Kongsberg Seapath 380 system with a Real Time Kinematic (RTK) correction by means of a ground control station located near the harbor, providing centimeter accuracy. The multibeam data were processed using Caris H&S hydrographic software to obtain high-resolution Digital Elevation Models (DEMs) corrected through tide gouge correction (https://www.mareografico.it/), sound velocity profilers, patch tests, and the application of statistical and geometrical filters to remove coherent/incoherent noise (Bosman et al., 2015). The soundings were merged and gridded for the generation of high-resolution DEMs (Fig. 1a). A 2016–2021 residual map was generated by means Global Mapper geographic software to differentiate current sectors of deposition and erosion in the Po Delta and prodelta slope (Fig. 1b).

The 8 sites of grab sampling were accurately selected based on the high-resolution (0.5 m cell size resolution) multibeam and backscatter data of the Po River Delta and prodelta slope (Fig. 1). Sediments were sampled along a river mouth-basin transect following the direction of bedforms progradation (i.e. southeastward direction; Bosman et al., 2020): from the

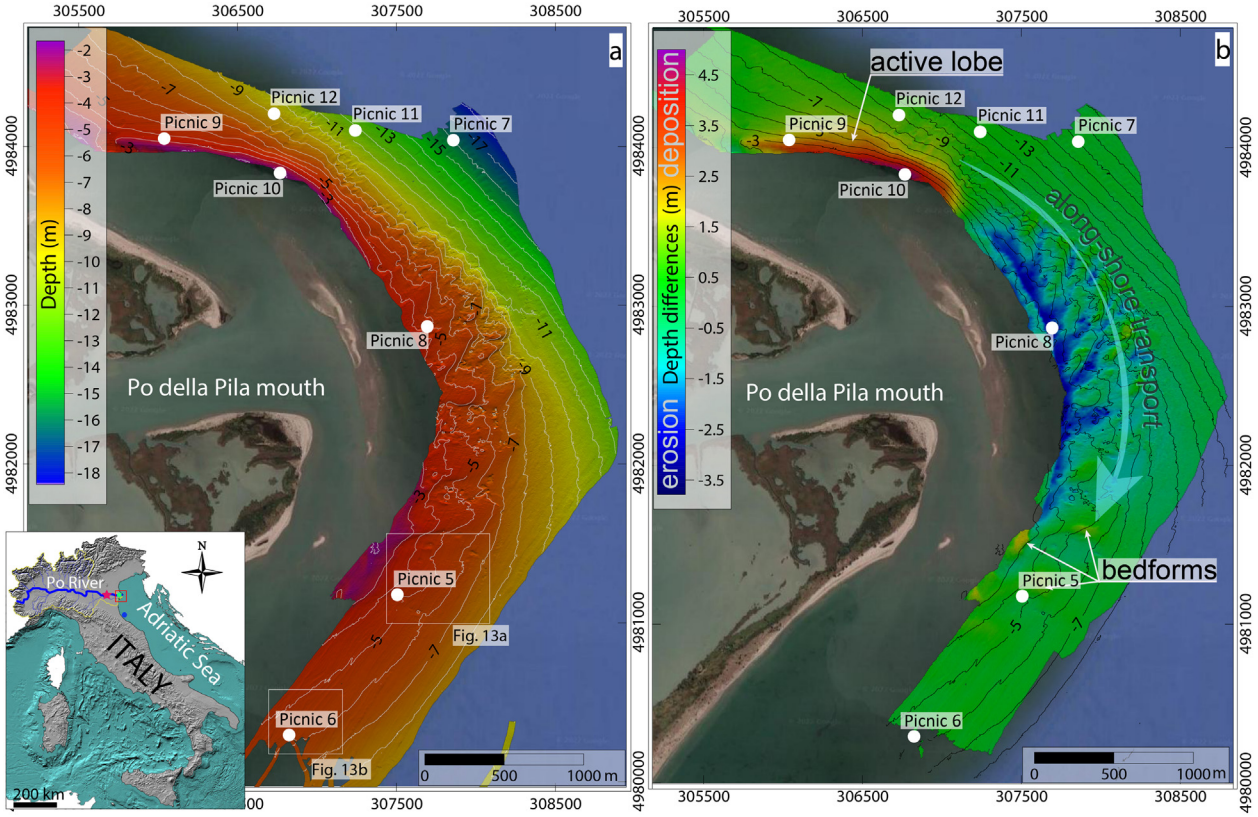

Fig. 1. a) Location of the sampling stations in the Po River prodelta acquired during the Picnic2021 survey. b) The residual map of the Po River Delta and prodelta slope generated from the high-resolution bathymetries. Inset shows the Italian peninsula with the surveyed area (red square), the location of the gauging station at Pontelagoscuro (red star), the farthest downstream gauging station at Cavanella (green dot), and the Nausicaa buoy offshore (blue dot).

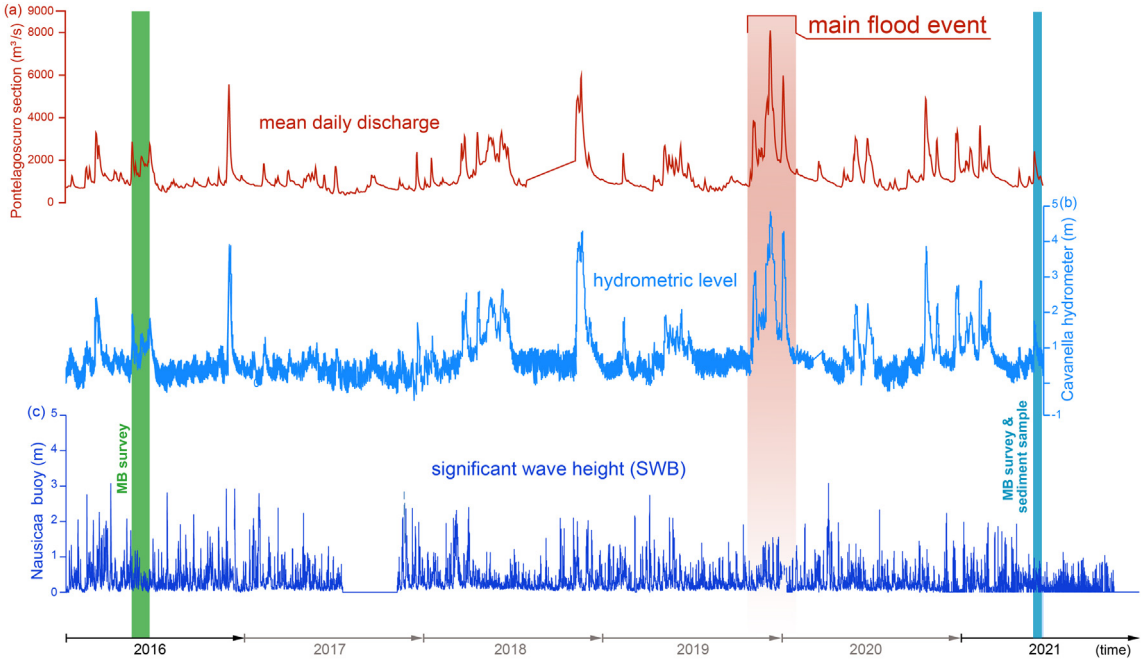

Fig. 2. River discharge and wave conditions at Po di Pila mouth for the interval encompassing the two bathymetric surveys offshore (2016–2021): (a) mean daily discharge at closure point (Pontelagoscuro); (b) hydrometric level near the delta outlet (Cavanella); and (c) significant wave height (SWB recorded by Nausicaa buoy). Since the 2016 multibeam survey, the major river flood in terms of discharge (discharge above 5000 m^3/s) and duration (20 days) is recorded in 2019. This event represents the most rapid change in delta geomorphology.

Table 1
List of samples, geographical coordinates (dry mass/wet mass = 100 - %).

Sample I·D.	Lat N	Long E	Depth (m)	Mouth distance (m)	Traveling distance (m)	Volume (ml)	Humidity (%)	dry mass (g)	Sand (%)	Mud (%)	D50 (mm)
Picnic 5	44.95796	12.55944	4.60	1074	5717	14	52	9.1	86.4	13.6	191.7
Picnic 6	44.94909	12.5499	5.96	2411	6834	14	50	9.5	85.6	14.4	142.6
Picnic 7	44.98378	12.56281	16	1797	2366	14	92	1.6	13.5	86.5	17.96
Picnic 8	44.97083	12.56111	2	1206	2657	30	70	12.7	76.6	23.3	22.82
Picnic 9	44.98338	12.53975	2.50	1486	1486	30	68	13.5	85.6	14.4	405.1
Picnic 10	44.98163	12.54907	2.29	1138	1138	30	73	11.3	54.8	45.2	95.03
Picnic 11	44.98417	12.55496	12	1517	1745	50	51	34.9	20.5	79.5	21.17
Picnic 12	44.98498	12.54845	9	1509	1509	35	61	28.8	20.2	79.8	24.62
Tot						217		121.4			

active delta lobe (Picnic 9 and 10; Fig. 1) to its distal reaches (Picnic 12, 11, 7: Fig. 1), and from migrating bedforms in the down-current side of the delta mouth (Picnic 5, 6 and 8; Fig. 1). In particular, and from North to South, Picnic samples 9 and 10 were retrieved at the active delta lobe at 2.5 m water depth. Samples 12, 11, and 7 were acquired at the distal reaches of the delta along a down-current transect between 9 m and 11 m water depth, sample 8 has been acquired in scour adjacent to the river bar at 2 m water depth. Finally, samples 5 and 6 were retrieved from bedforms in the down-current sector of the delta at 4.5 m and 6 m water depth, respectively (Fig. 1). Sediment samples were collected from each station using a Van Veen grab of 25 l that allows the recovery of ca. 60 kg (considering an average density of 2.5 g/cm^3) of sediment. Sub-samples were then stored in 0.5-l pre-combusted glass bottles at −20 °C.

2.3. Sediment and grain size analyses

Granulometric analysis and determination of the water content were carried out by taking aliquots of sediments, from each sampling station. Approximately a spoon of wet sediments was weighted with an analytical balance with mass measured to two decimal places. Then the sediments were dried at 50 °C for 24 h, weighted again, and the ratio of wet to dry sediment mass was measured. Grain size was determined using a Malvern Mastersizer 3000 analyser (Hydro EV) for size ranges from 0.01 to 3500 μm fraction of the Geohazard core laboratory at CNR-ISMAR, Bologna (Table 1). Sediment samples were dispersed into demineralized water for 24 h and subjected to ultrasounds for 60 s before starting the analysis. Laser-scattering spectra has been processed using the Multiple Sample Statistics sheet in the Excel worksheet GRADISTAT (Blott and Pye, 2001). Grain-size analysis accounts for all particles included in the sample and are reported on the Wentworth scale (Wentworth, 1922).

2.4. Sediment provenance based on XRF analysis

Geochemical analyses were conducted on sediments, to assess provenance. Major and trace elements were analyzed by X-Ray fluorescence (XRF) on 3 g. powder pellets, using a Panalytical Axios 4000 spectrometer. Accuracy and precision rely on a systematic analysis of standards. For major elements (expressed as weight %) they are better than 3 %; for trace elements (expressed by mg/kg) they are better than 10 %. The matrix correction methods follow Franzini et al. (1972), Leoni and Saitta (1976), and Leoni et al. (1982). For the reconstruction of sediment provenance, bulk sediment geochemical analyses of river deposits from earlier studies were used for comparison with data obtained from this study. Alpine and Apennine rivers carry unique geochemical signals that reflect distinct catchment geology: for a comprehensive summary of geochemical characteristics, the reader is referred to Amorosi et al. (2022). The Po River drainage basin includes the Western and Central Alps, and the Ligurian-Emilian section of the Northern Apennines. Large outcrops of metamorphic and mafic-ultramafic intrusive rocks (ophiolitic complexes) are the diagnostic feature of the Western Alps. In the Ligurian-Emilian Apennines shales, marls and sandstones are widespread, with the local presence of ophiolitic rocks (Amorosi et al., 2022). This ultramafic signature is confirmed by relatively high Cr and Ni values, as a distinguishing feature of Po River sediments (Fig. 3).

2.5. Microplastic extraction

For the determination of the MPs concentration, two different extraction protocols were applied: one was devoted to the isolation of large MPs (particles in the 5.0–0.5 mm range) and the other one to small MPs (particles < 0.5 mm). Briefly, for large MPs an aliquot of 30 g of dried sample was scrutinized under stereomicroscope (Leica M50 with a cold light source Leica KL 300 LED, Leica Microsystems) and all the suspected plastic particles and fibers were counted, photographed, and described in detail by annotation of color, shape and size (Fig. 4). The visual identification was performed based on the morphological properties of the surface, following the guidelines of Gago et al. (2020). The categorization included four shape classes: (i) fragment, (ii) fiber, (iii) filament, (iv) film and (v) other types (spongy particles and spheres). Filaments with a smaller diameter than fibers were present as tangles. We considered 5 classes of color: (i) blue, (ii) brown, (iii) white, (iv) orange, (v) gray. All the suspected plastic particles were then removed and submitted to μFTIR analysis of identity confirmation.

Analysis of small MPs (0,5–0,005 mm) was carried out on 5 g aliquot from each sample, following a density separation protocol (Quinn et al., 2017; Stile et al., 2021). Briefly, the sediment aliquots were treated with hydrogen peroxide at 30 % and filtered onto a 5 μm pore size stainless steel filter (Paco filter GMBH, Steinau Germany). The fraction retained onto the filter was then washed with ultrapure water and submitted to density separation by using $ZnCl_2$ solution (1.7 g/ml density). The obtained mixture was transferred into a glass separation funnel specifically designed for enabling the plastic separation procedure, stirred with an orbital shaker (50 rpm) for 3 h at room temperature, and then left to settle for 12 h. After that, the dense sediment settled on the bottom of the separation funnel were rinsed off by opening the system through the stop cock, and collected in a glass beaker. The low-density fraction, containing the targeted plastics floating in the supernatant of the solution, was retained in the separation funnel instead and the stop clock was closed to avoid its loss. This fraction was then discharged into a second glass beaker via the tap at the bottom by decanting through addition of fresh $ZnCl_2$ solution. To ensure that any of the particles adhered to the separatory funnel glass wall was recovered, a second portion of fresh $ZnCl_2$ solution was added in the empty funnel and the procedure was repeated twice. Moreover, the sediments rinsed at the first step of the separation procedure, were submitted again to the same extraction procedure (thus replicated) in the same separation funnel to ensure complete recovery of the plastic particles from the original matrix. All the supernatant collected fractions were then filtered over a Whatman® GF/C filter (47 mm diameter; 1.2 μm pore size). The filter was then submitted to micro-FTIR analysis for polymer identification. For further detail regarding the method optimization and recoveries please refer to our previous paper (Stile et al., 2021).

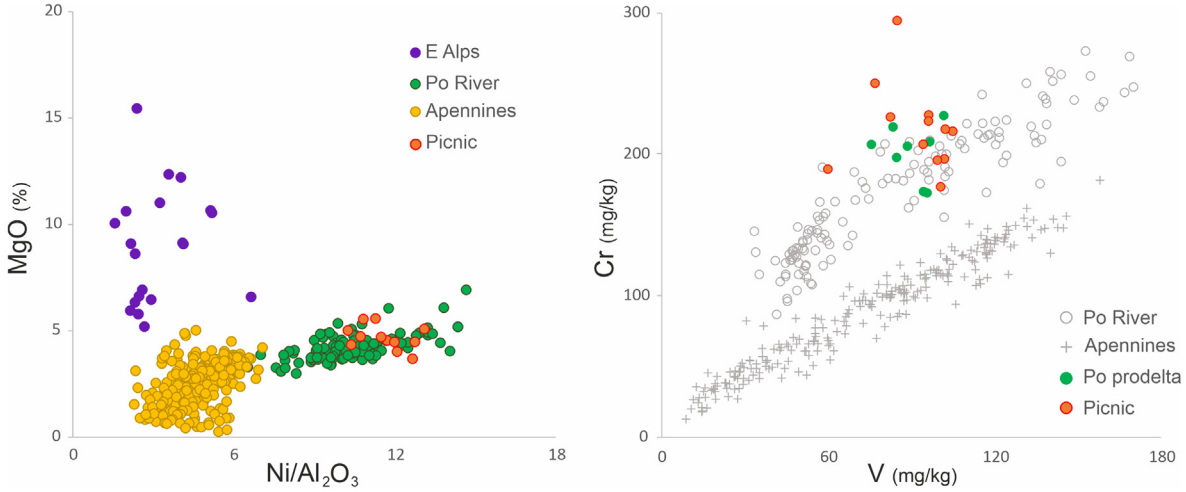

Fig. 3. Scatterplots of Mg-Ni/Al_2O_3 and Cr/V and sediment provenance interpretation of "Picnic" samples. High Cr/V and Ni/Al_2O_3 ratios correspond to sediment sourced from the ophiolite-rich Po River catchment and traveled for a longer distance.

2.6. Microplastic characterization by micro-FTIR

MPs characterization was carried out by micro-Fourier Transform Infrared Spectroscopy, using a Spotlight 200i FT-IR (Perkin Elmer), equipped with a micro ATR diamond crystal, according to the procedure described in Saliu et al. (2021). For each particle 32 scans in the 3600–600 cm^{-1} range with 4 cm^{-1} resolution was acquired. Spectra were compared to reference spectra available in a commercial library (Hummel polymer library) by using the patented COMPARE™ spectral comparison algorithm provided in the Perkin Elmer Spotligh II instrument software (Perkin Elmer). A positive identification with the reference library was assigned for matches ≥70 % according to the indication of the Guidance of Marine Litter in European Seas of the European Commission (Galgani et al., 2013).

Small microplastic particles were counted in three subfields of the filter surface (covering 10 % of the total filter surface) and the concentration in the sediments was determined by upscaling and considering the dry mass of the original core samples. To evaluate cross-contamination, controls were run in parallel during the entire sample treatment procedure and averages of fragments and fibers in procedural blanks were subtracted from sample particle counts. Values were expressed as items in kg of dry sediment to compare with other studies. In this work, we did not consider cellulose fibers in our counts (both "synthetic" and "natural") due to the difficulty of providing clear discrimination by μFTIR spectroscopy. Examples of detected plastic particles with relative spectra are reported in Fig. 5.

2.7. Phthalate analysis

PAEs analysis were carried out by employing the method described by Paluselli et al. (2018). Before the analysis, an aliquot of 10 g from each sediment sample was collected and freeze-dried for 12 h, grounded and sieved through a 200 μm mesh screen. The aliquot was spiked with DnBP-d4 and DEHP-d4 used as labeled internal standard and homogenized using a glass stick. Extraction was carried out by using an ultrasonic bath (40 W, no heating) in 3 ml of acetone. Each sample was extracted three times for 15 min. After 5 min of centrifugation at 25 °C and 4000 rpm, the extracts were purified through a Pasteur pipette filled with combusted quartz

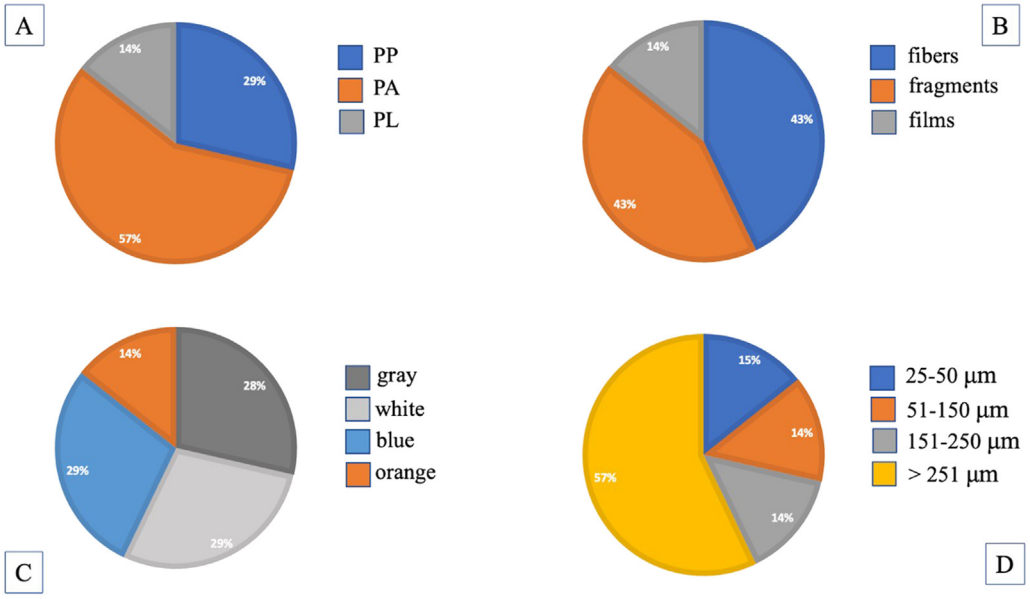

Fig. 4. Microplastic distribution in terms of (A) polymer type (PP = polypropylene; PA = polyamide; PL = polyester), (B) shape (fibers, fragments, films), (C) color (gray, white, blue, orange) and (D) size (25–50 μm, 51–150 μm, 151–250 μm, >251 μm).

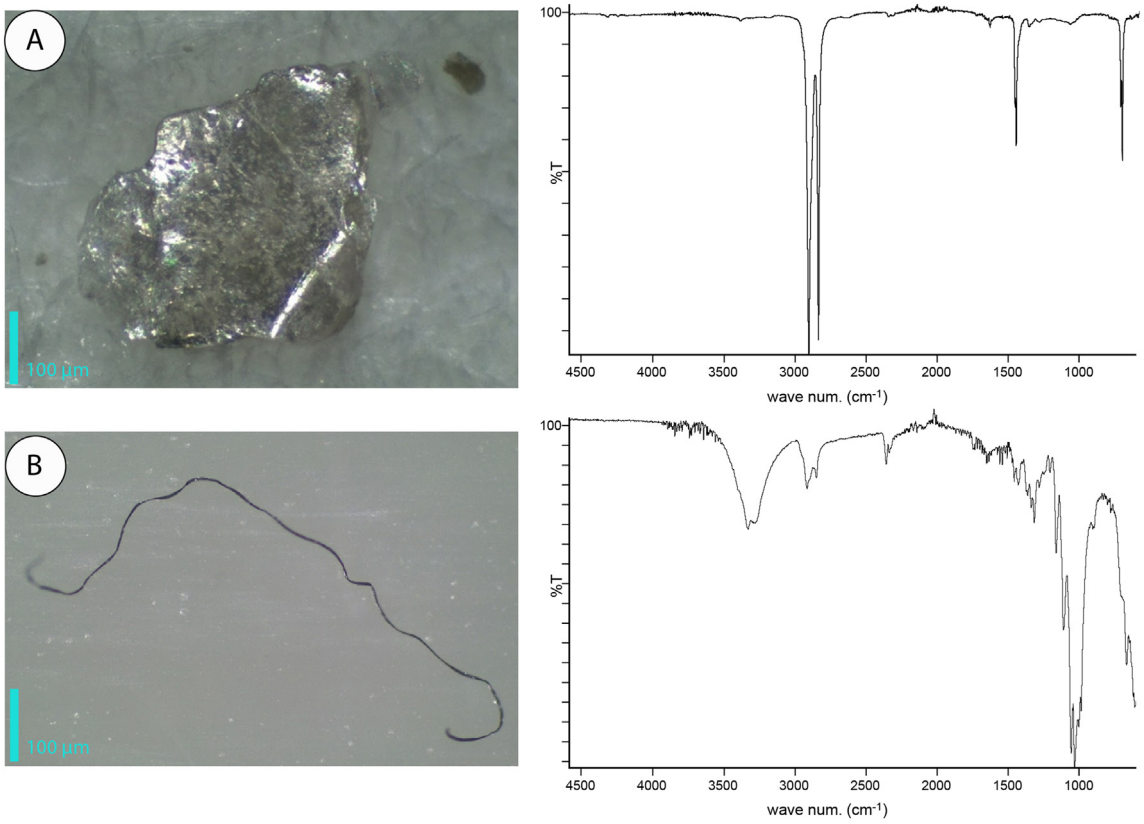

Fig. 5. Examples of the detected particles with associated spectra acquired with µFTIR: A) polyethylene fragment and B) cellulose fiber.

wool, transferred into a vial and concentrated to a final volume of 250 µl under nitrogen steam and diluted in ultrapure water: methanol 80:20. Analysis was carried out by employing a Thermo Fisher TSQ quantum access max instrument. Tandem mass spectrometry transitions for the selected PAEs were set up as indicated in Saliu et al. (2020). Specifically, the researched PAEs were: Dimethyl phthalate (DMP); Diethyl phthalate (DEP); Diisobutyl phthalate (DIBP); Dioctyl phthalate (DOP); Butyl benzyl phthalate (BBzP); Dihexyl phthalate (DHP); Di-2-ethylhexyl adipate (DEHA); Di(2-ethylhexyl) phthalate (DEHP); Dicyclohexyl phthalate (DCHP) Diisononyl phthalate (DiNP); Diisodecylphthalate (DiDP).

2.8. Quality assurance

In order to avoid contamination, particle isolation procedure, and PAEs extraction were carried out in a dedicated ISO 6 clean room laboratory, following all the common precaution prescribed for MPs analysis (GESAMP, 2016) i.e. checking airborne contamination by filter analysis, the use for sample manipulation of only glass material previously baked at 400 °C, the rinsing of all the equipment with distilled water daily checked by filtration and infrared analysis, the covering all the equipment with aluminum, the use of only 100 % natural fiber laboratory coat and clothing. The possible secondary contamination that usually occurs in microplastic and phthalate studies also during sampling operation (Shruti and Kutralam-Muniasamy, 2023, Saliu et al., 2022) was controlled by running opportune field and procedural blanks. Specifically, three field-level blanks were set aside during sample collection: one at the beginning of the sample operation, one in the middle and one at the end. These blanks were obtained by employing the same grab used for sediment collection that was left to the open air for 1 h on the boat and then washed with 2 l of MilliQ water. An aliquot of the drained water was collected on 0.5 l bottles similar to those used for the sediment collection. Moreover, six procedural blanks were run in the cleanroom employed for the real sample. In this case all the same procedures adopted for the isolation of the microplastic and phthalates from the sediment were run by starting from bottles similar to those used for the sampling, that were in this case preliminary washed with MilliQ water and left inside the cleanroom. The procedural blanks were used to assess the limit of quantitation of the method (LOQ) defined as 10 times the standard deviation of the procedural blanks, while the field blank averages results were used for subtraction adjustments.

2.9. Statistical analysis

Results underwent statistical analysis to highlight possible significant differences among samples ($p < 0.05$). Specifically, the nonparametric Mann-Whitney *U* test was used to investigate variations in the concentration of microplastics and cellulose fibers among the different regions of the river mouth-basin transect, since, according to the Shapiro–Wilk test, data were not normally distributed. Spearman coefficient was measured to assess possible correlations between the concentration of plastic particles, of cellulose fibers and of phthalic acid esters (PAEs). Analyzes were performed using the software SPSS ver. 27 (IBM, New York). Multivariate analyses using principal component analysis (PCA) were performed by using the software XLSTAT (Addinsoft 2020). The data were first standardized by the variable mean and standard deviation. Correlation among variables and principal components (F) was quantified as the square cosine of their angle in the loading graph. For data visualization we selected the two principal components covering the larger percentage of total variance captured by all principal components.

3. Results

At the Po River mouth recurrent changes of geomorphological features reflect short-term sedimentological evolution of the mouth bar and prodelta slope. The following paragraphs describe these features highlighting sediment distribution and lateral extent of lithosomes resulting from the 2019 river flood event. Sampling stations were selected by integrating

morpho-bathymetric analyses with the residual time-lapse map denoting sectors of main deposition and erosion from the 2016–2021 (Fig. 1). Sediments from each sampling station have been analyzed defining their provenance and characterizing pollutant concentration and particle characterization.

3.1. Morphobathymetry

The Po River prodelta is characterized by a gradient that changes seawards from ~0° to 8° to 0.6° from the river mouth to the prodelta slope based on the bathymetric map of 2021 (Fig. 1). The main subaerial break in slopes (i.e., rollover point sensu Pellegrini et al., 2020) typically occurs in <3 m-deep waters. The main morphological features highlighted by the bathymetry is the deposited lobe situated at <3 m water depth (red scale in Fig. 1b). The lobe is highly asymmetric and is skewed toward the south compared to the river mouth. The main depocenter of the lobe is located in the northern sector (up-current sector) and extends over a surface of about 1 km^2 where it reaches a maximum thickness of 4.5 m. Here sediments are mostly sandy with up to 86 % of sand-size particles (Picnic samples 9 and 10, Table 1). The total sediment volume of the lobe (positive residual with respect to the 2016 survey) is about +1.3 Mm^3 and can be considered as the most active bedform, because it accumulated most of the sediment discharged during the 2019 flood event. The lobe thins seaward along the coast to <1 m. Concurrently, samples show a decreasing content in sand-size particles from 20 % (samples 11 and 12) to 13.5 % (Picnic 7; Table 1). In the southern sector, meter-scale bedforms of reduced extent (300–500 m long and ca. 1 m high, with a wavelength of ca. 100 m), form between 5 and 10 m of water depth (Fig. 1). These bedforms (referred to as transverse bars in Bosman et al., 2020) are oriented at ca. 20° and 60° relative to the coast strike in the down-current sector (Fig. 1). The bedforms are characterized by sandy sediment with up to 86 % of sand-size particles (samples 5 and 6, Table 1). Adjacent to the mouth bar, the main erosional sector is represented by a ca. 30 m wide and 2 m deep scour oriented parallel to the coast (Fig. 1). Smaller scours perpendicular to the coast are superimposed to the bedforms (Fig. 1). Here sandy sediment dominates, reaching 77 % of the particles (Table 1).

3.2. Sediment provenance

Geochemical analyses from the Picnic samples were compared with previously published data from Alpine, Apennine, and Po River catchments (Fig. 3). Among the diagrams that best allow the discrimination of sediment provenance, we used the Mg vs Ni/Al_2O_3 plot and the Cr/V diagram. High Ni/Al_2O_3 and Cr/V values reflect the presence of ophiolites in the drainage basin and trace the Po River provenance, while high Mg contents are the typical geochemical signature of rivers draining the Eastern Alps (Amorosi et al., 2022 for a review). Apennine fluvial deposits, instead, are characterized by low values of both indicators. In both diagrams, Picnic samples show Ni/Al_2O_3 values in the range of 10–13 and a relatively high Cr proportion (>175 mg/kg) that clearly overlaps the composition of Po River sediment, with locally higher Cr values (Fig. 3). Picnic samples plot in the same field as Holocene Po prodelta muds from a sediment core recovered close to the Po River mouth (Fig. 3). Geochemical data suggest a marked Po River provenance, with no significant contribution from other (Eastern Alpine and Apennine) fluvial sources. This suggests that sediment travels for hundreds of km across the Po plain before reaching the river mouth (source-to-sink).

3.3. Microplastic identification using μFT-IR

A total of 256 suspected plastic particles were identified by the stereomicroscope (Leica® S9E Leica Microsystems GmbH, Germany) and characterized by μFT-IR (Fig. 4). For 145 particles (57 %) the plastic polymer type was identified. Calculations were carried out on confirmed plastic items. Considering the morphological appearance 43 % of the detected plastic items were classified as fibers, 41 % as fragments, and 19 % as films (25 %; Fig. 4B). Concerning the constituting polymers (Fig. 4A), 57 % of the particles resulted composed by polyamide (PA), 29 % polypropylene (PP) and 14 % polyester (PL). Fibers were mostly polypropylene (PP) (67 %), followed by 33 % polyester (PL). In terms of size distribution, most of the microplastics (57 %) were larger than 251 μm, while 15 % were within the 25–50 μm size range, 14 % between 51 and 150 μm and 14 % were 151–250 μm in size (Fig. 4D). Considering colors (Fig. 4C) 29 % of the detected items was blue, 29 % white, 28 % gray, and 14 % orange (14 %). Overall, microplastics resulted to occur in 4 (50 %) out of 8 samples with an average concentration of 139.7 ± 80 MPs/kg d.w. The maximum concentration of 625 MPs/kg d.w. was detected in sample Picnic 7 (Table 2). In samples Picnic 8, 9, 10 and 12 no microplastics were found instead. More details about particle characterization are provided in the supplementary material associated to this paper. Statistical analysis carried out by grouping samples on the basis of geomorphology of the related sampling point showed no significant differences between the concentration detected in the active lobe (Picnic 9, 10), in the distal reaches of the lobe and the migrating bedforms (Picnic 5, 6, 7, 8 11, 12) (Mann Whitney U test = 2, ρ = 0.115), and among migrating bedforms (Picnic 5 and 6) and distal reaches of the active lobe (Picnic 7, 8, 11, 12) (Mann Whitney U test = 2, ρ = 0.348) (Fig. 6).

3.4. Detection of cellulose fibers

Micro-FTIR analysis showed that 94 % of all the detected fibers were composed of cellulose (Fig. S1). More specifically, cellulose fibers were found in 100 % of the 8 samples with an average concentration of 2262.5 ± 338 fibers/kg d.w. of sediment. Table 3 and Fig. 7 reports the cellulose fiber distribution as fibers/kg d.w. in the different samples. The highest concentration was found in sample Picnic 8 (3800 fibers/kg d.w.), while the sites displaying the smaller amounts were Picnic 5 and 12 (1300 fibers/kg d.w and 1304 fibers/kg, respectively). Regarding colors, 91 % of the fibers were classified as white transparent, 1 % yellow, blue %, brown 1 %, black 2 % red 2 %.

Table 3 also reports the fiber distribution among the 5 size classes in all the analyzed samples (class 1: ≤0.5 mm, class 2: 0.51–1.0 mm, class 3: 1.0–2.0 mm, class 4: 2.1–4.0 mm, class 5: ≥4.1 mm). In four samples the smaller fibers were predominant with respect to the larger ones (Picnic 5 Picnic 6: 700 fibers/kg d.w. 0.51–1 mm in size; Picnic 8: 1000 fibers/kg d.w. ≤ 0.5 mm in size; Picnic 11: 700 fibers/kg d.w. 0.51–1 mm in size), following the power law distribution coherent with a 1-D fragmentation model (Cózar et al., 2014; Fig. S2). In Picnic 10 and Picnic 12, fibers were mostly within 2.1–4.0 mm (1100 fibers/kg d.w., 500 fibers/kg d.w.), while in, Picnic 7 and Picnic 9, fibers mostly ranged between 1.1 and 2 mm (400 fibers/kg d.w., 2200 fibers/kg d.w., 800 fibers/kg d.w.; Fig. S2). Log scaled Relative abundances of Fiber considering sizes are plotted in (Fig. 8). Statistical analysis showed significant differences for fibers abundance (fibers ≤ 0.5 mm) in the active lobe (Picnic 9 and 10), the distal reaches of the lobe and the migrating bedforms (Picnic 5, 6, 7, 8, 11, 12) (Mann Whitney U test = 2, ρ = 0.039) (Fig. 9). No significant differences

Table 2
Concentration of microplastics in items/kg d.w., distinguished in fibers and non-fibers.

Sample	Non fibers/kg d.w.	Fibers/kg d.w.	MPs tot/kg d.w.
Picnic 5	219.8	109.9	329.7
Picnic 6	105.3	0	105.3
Picnic 7	0	625	625
Picnic 8	0	0	0
Picnic 9	0	0	0
Picnic 10	0	0	0
Picnic 11	28.7	28.7	57.4
Picnic 12	0	0	0
Mean	44.2	95.45	139.7
S.E.	28	77	80
Mean in contaminated samples	117.9	254.5	279.4
S.E. in contaminated samples	34	114	92

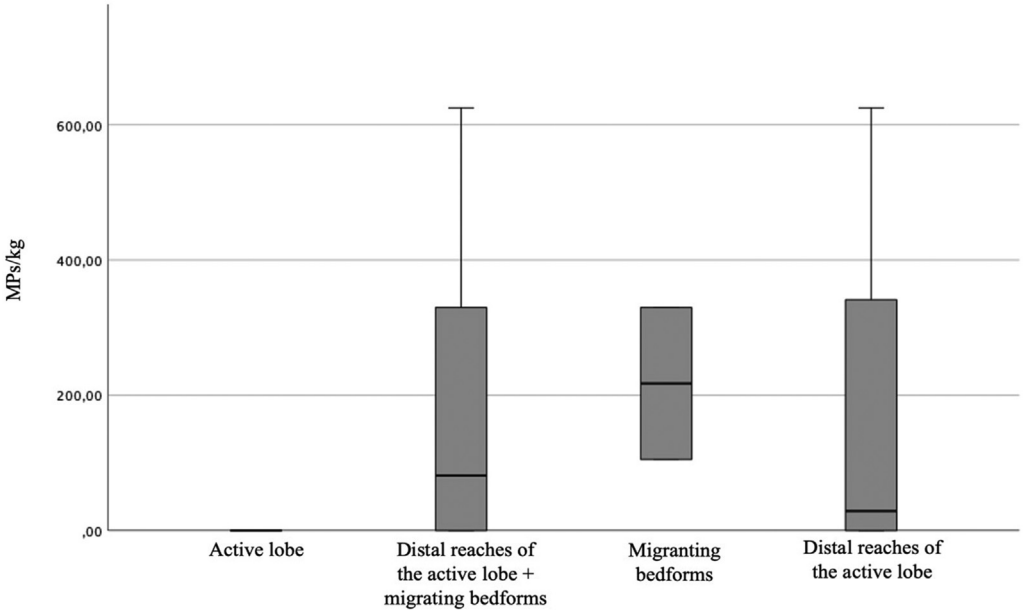

Fig. 6. Box Plot related to the MP distribution. No significant differences were observed between the different sampling locations ($p > 0.05$).

among the slope of the logscaled distribution were highlighted (the active lobe, the distal reaches of the lobe and the migrating bedform Mann Whitney *U* test = 2, ρ = 0.182; the distal reaches of the lobe vs migrating bedforms Mann Whitney U test = 3, ρ = 0.643) (Fig. 10).

3.5. Phthalates

LC-MS/MS analysis showed the occurrence of phthalates in all the samples (Table S1) with concentration for the sum of phthalates ranging from trace amounts to a maximum of 34.9 ng/kg d.w found in sample Picnic 10. The average concentration for the sum of phthalates resulted i 13.7 ± 11.1 ng /kg d.w. The most abundant congener was DEHP with a maximum of 29.5 ng/kg d.w. Statistical analysis showed no significant differences among the concentrations retrieved in the different sampling stations.

3.6. Multivariate statistical analysis

The dataset including MP, cellulose fiber and phthalate concentrations and a series chemo-physical descriptors of the sediment samples (including sediment density, D50, % sand, % mud, and water content) and geographical descriptors of the sampling station (mouth distance, traveling distance and sample depth), was submitted to principal component analysis (PCA) in order to reduce the dimensionality of the data set, spot outliers, highlight key variables and identify possible clusterization in the data. The rho Spearman coefficient was used to highlight correlations in data. Table S4 reports the details of the correlation matrix obtained after application of the first variables selection (Supplementary files attached to the paper). A correlation assay was carried out by considering microplastic and cellulose fiber concentrations, under the testing hypothesis that fibers can serve as a proxy for the sedimentation process of microplastic. No correlation was found for the total cellulose fiber and the total MP concentration (rho = 0.964, alpha = −0.09). Noteworthy, a significant correlation was found to occur between the total MP concentration and cellulose fibers in the size range 2.1–4 mm (rho = −0.719, alpha = 0.044) instead. The same correlation was highlighted by considering t MPs and cellulose fibers counts (rho = −0.802, alpha = 0.017). Correlation researched by considering sediment descriptors showed a significant correlation between the total fiber concentration with humidity (rho = 0.857, alpha = 0.007), fibers 1.1–2 mm in size with humidity (rho = 0.916, alpha = 0.001), and between sand content and depth (rho = 0.838, alpha = 0.004) PCA results are reported in Fig. 11. As depicted the two principal components of the PCA explained 57.45 % of the total variability (Fig. 11). Considering the loadings plot, Picnic 5 and Picnic 6, appear clustered together and are sharply separated by the other samples. Considering the scores plot, traveling distance appears as the most relevant variable in the class separation between samples influenced by the gyre and those not (34 % of contribution to the PC1), followed by mouth distance (21 % of contribution to PC1) and MPs concentration (13 %). Samples retrieved from stations that are not expected to be influenced by the gyre display clustered data: Picnic 8 and Picnic 10 characterized by higher fibers content and prevailing sand content and Picnic 11 and 12 forms a distinct cluster determined by higher mud content and microplastic content from. More specifically, samples Picnic 5, 6 and 7 are highly scattered along the PC1 displaying highly negative and highly positive scores, respectively. These scores are determined mostly by different values of traveling distance. Picnic 7 scores positive values due to the high amount of MPs/kg. Samples Picnic 8, 10 11, 12 are scattered along PC2 where the main contribution to the variable is determined by mud content, sample depth, mouth distance. Specifically samples 11 and 12 are characterized by high values of mouth distance and water depth, high mud content and low fiber content and higher MPs content, whereas samples 8 and 10 are separated in a different cluster and are characterized by a minor distance from the mouth, higher content of sand

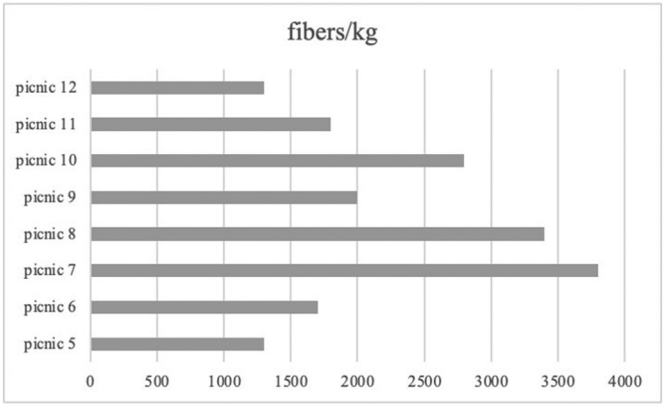

Fig. 7. Concentrations of the cellulose fiber in the different sampling stations of the Po della Pila Mouth in terms of fibers/kg.

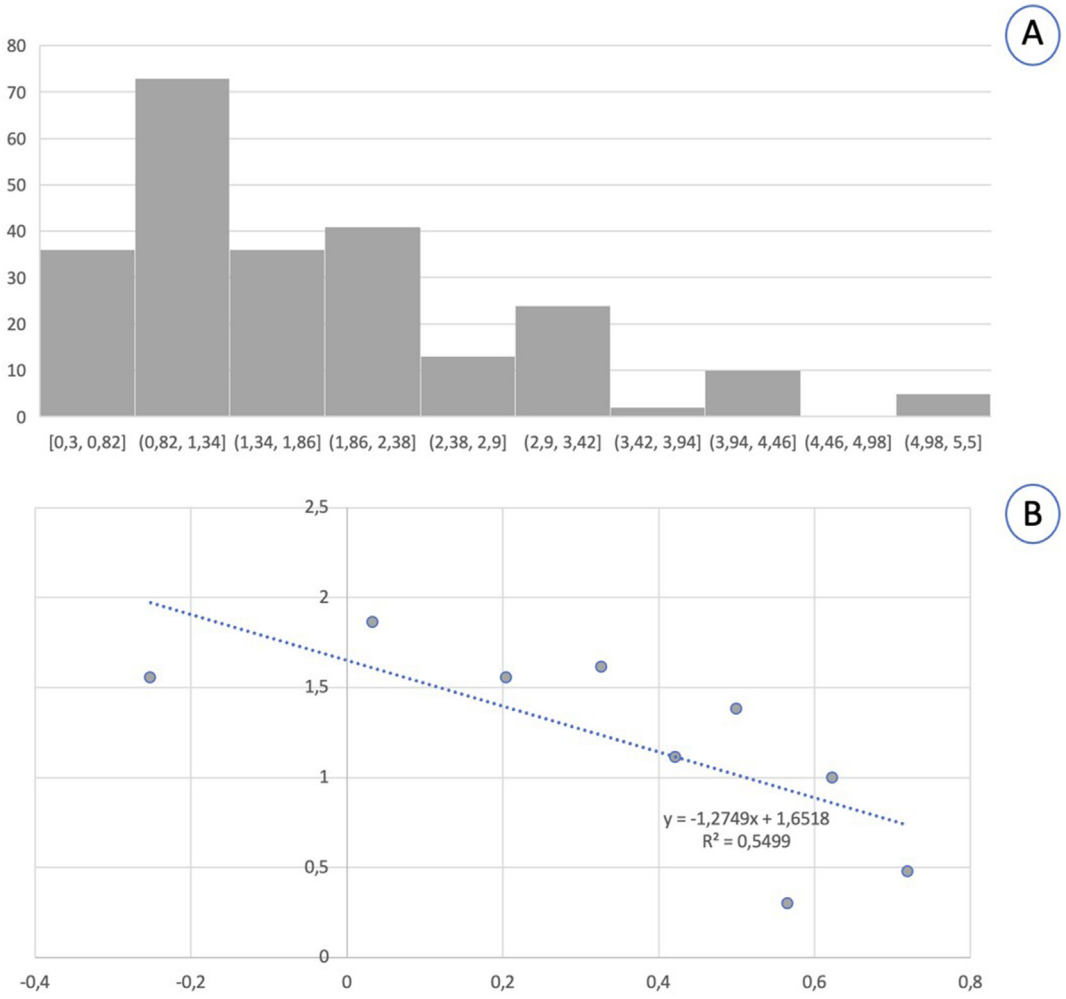

Fig. 8. A) Size distribution in abundance of cellulose fibers in the Po della Pila sediments B) size distributions of normalized abundance in logarithmic scale.

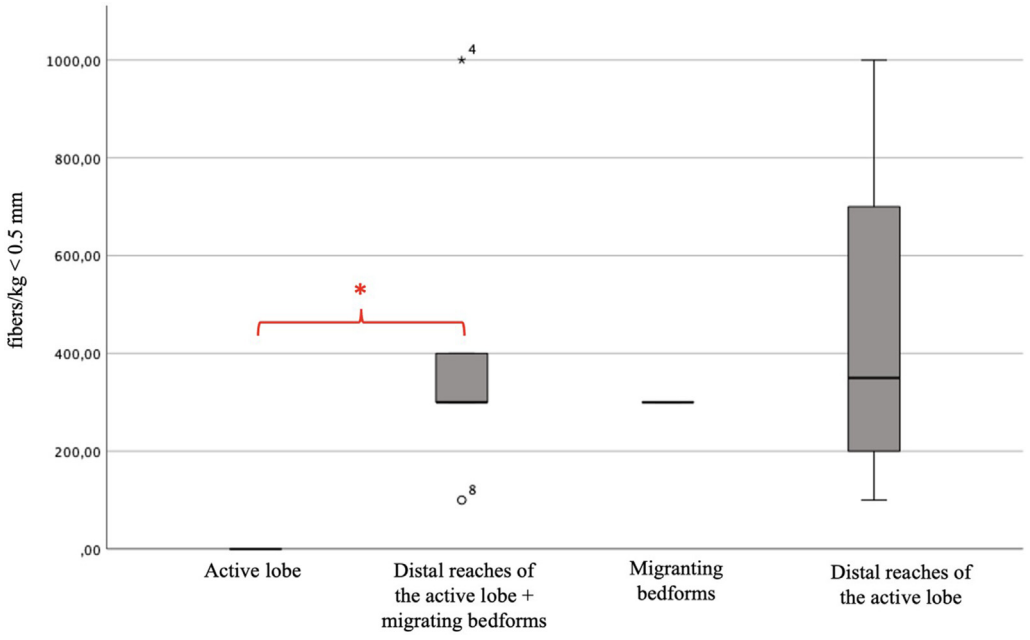

Fig. 9. Box Plot related to the fibers < 0.5 mm distribution in the sampling point classes. A significant difference is highlighted among younger lobe and prodelta + migrating bedforms ($p < 0.005$).

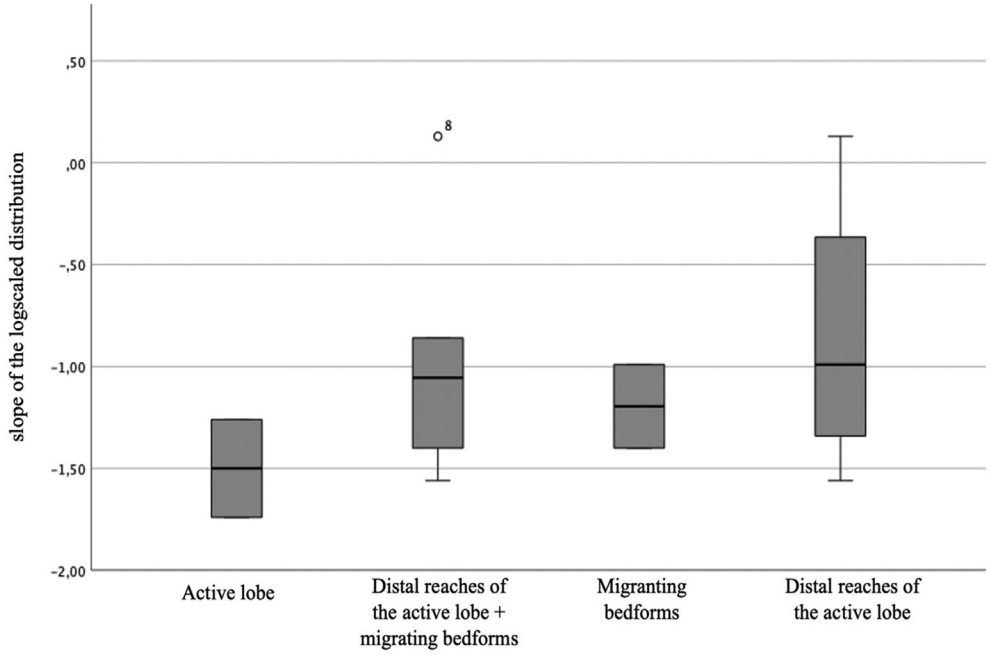

Fig. 10. Box Plot related to the slope of the logscaled distribution according to Cózar et al. (2014). No significant differences were highlighted between the different sampling locations ($p > 0.05$).

and higher levels of fiber (Fig. 11) Finally, sample 7 resulted an outlier due to the high fiber content and the relatively high depth (thus the exceptionality is related to higher fiber abundance in the distal reaches). Interestingly, fibers resulted significantly correlated to the humidity content of the samples, while no other significant correlations was highlighted in the descriptors dataset.

4. Discussion

4.1. Microplastic sequestration in the prodelta benthic sediment

Most river deltas worldwide display prominent subaqueous prodeltas, representing the main locus of sediment deposition and a potential archive recording anthropogenic signals through time (Syvitski et al., 2022; Pellegrini et al., 2020; Trincardi et al., 2023). Flood events are the key processes under which large amounts of sediment and pollutants are delivered from the continent to the prodelta systems (Rech et al., 2014; Lebreton et al., 2017; Schmidt et al., 2017). Accordingly, in recent times there has been a significant increase in the scientific literature concerning the role of rivers in polluting the oceans with plastic litter (Van der Wal et al., 2015; Weiss et al., 2021). The source-to-sink approach applied in sedimentological research can help to elucidate land-to-sea transport and burial dynamics, aimed at identifying the sources and pathways by which MPs are mobilized and moved throughout natural habitats they may severely impact, including those in which they are ultimately sequestered (Kane and Fildani, 2021). Table 4 reports the current available scientific literature regarding the Northern Adriatic Sea. Recent estimates from the surface waters, sampled in 2019, reveal an annual load of floatable plastic particles of 145 tons (Munari et al., 2021), highlighting the need to understand how much of those particles are retained in the Po Delta system. In

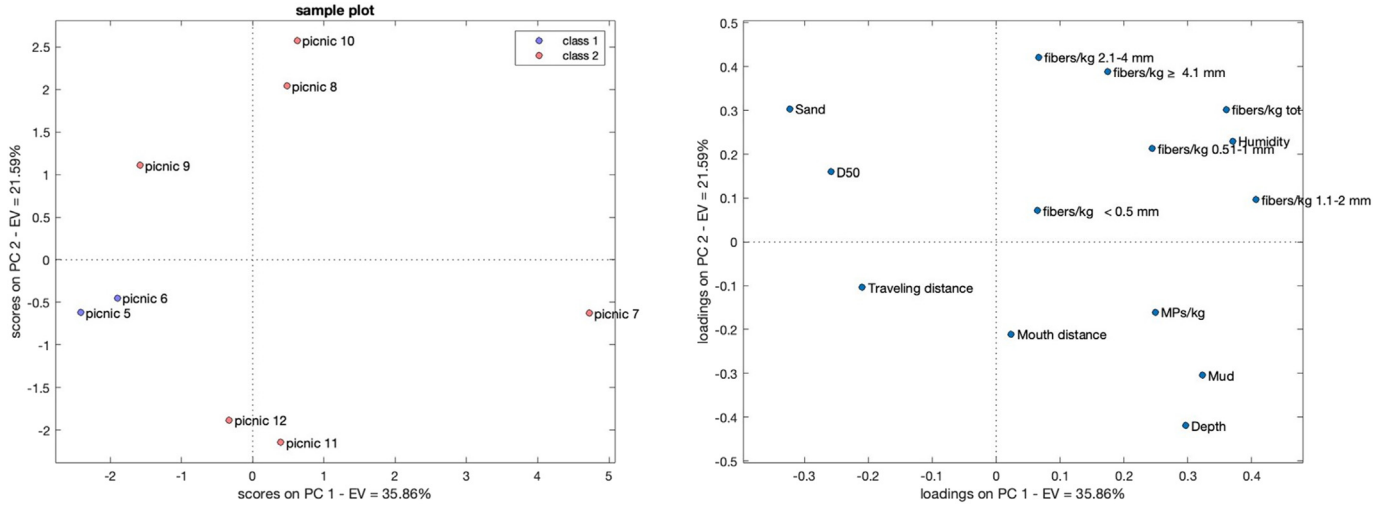

Fig. 11. Loadings and scores plot from the principal component analysis (PCA). PC1 and PC2 explained 57.45 % of the total variability. Class separation along PC1 is mainly influenced by the traveling distance variable.

Table 3
Cellulose fiber total concentrations and for each size class (<0.5 mm, 0.51–1 mm, 1.1–2 mm, 2.1–4 mm, ≥4.1 mm) in the different sampling locations expressed in fibers/kg.

Sample I.D:	Fibers/kg < 0.5 mm	Fibers/kg 0.51–1 mm	Fibers/kg 1.1–2 mm	Fibers/kg 2.1–4 mm	Fibers/kg ≥ 4.1 mm	Fibers/kg tot
Picnic 5	300	400	400	300	0.0	1300
Picnic 6	300	700	300	300	100	1700
Picnic 7	300	900	2200	400	100	3800
Picnic 8	1000	900	900	500	100	3400
Picnic 9	0.0	700	800	500	0.0	2000
Picnic 10	0.0	600	900	1100	200	2800
Picnic 11	400	700	600	200	0.0	1800
Picnic 12	100	300	400	500	0.0	1300

subaerial deposits of the Po Delta the maximum concentration found was 23.30 MPs/kg and 78.8 MPs/kg by Piehl et al. (2019) and Atwood et al. (2019), respectively, which point out the need to determine the abundance of MPs in the subaqueous counterpart of the delta. Our results on the Po prodelta sediment reveal a concentration of two orders of magnitude higher than those documented for the subaerial deposit with an average concentration of 139.7 ± 80 MPs/kg d.w., and a pick in MP abundance of up to 625 MPs/kg d.w. (Table 2). The higher concentration can be due to our lower range classes of 25–800 μm compared to the 1–5 mm used in the earlier documentation, since larger plastic items are expected to display a power-law size distribution with a scaling exponent from 1 to 3 (depending on the dimension of the plastic item) in the increase of the number of small size particles, being fragmented into smaller pieces due to photooxidative degradation and mechanical stresses (Cózar et al., 2014). However, it is worth mentioning that MP concentration documented in the benthic sediments are usually from one to two orders of magnitude higher than those found in sandy beaches (e.g. Horton et al., 2017; Hurley et al., 2018; Simon-Sánchez et al., 2019; Xiong et al., 2019). Finally, if we compare our result with one of the most polluted environments of the Northern Adriatic Sea, the MP abundances found in the Po prodelta are one order of magnitude smaller than the average concentration of 1445 MPs/kg found for the non-fiber 30–500 μm classes in the sediment of the Venice Lagoon detected (Vianello et al., 2013). This finding can be explained by the elevated and direct input of litter (Madricardo et al., 2017, 2019) with small water exchange rates, transport time, and mixing (Umgiesser et al., 2014) in a less energetic environment compared to the Po Delta (Maicu et al., 2018), such as the Venice Lagoon.

The majority of studies dealing with MP pollution have in fact targeted lakes (e.g. Sruthy and Ramasamy, 2017; Waldschläger et al., 2022) and wetlands (e.g. river thalwegs, estuaries, lagoons, mangroves sediment: Costa et al., 2011; Willis et al., 2017; Waldschläger et al., 2022) and very few in the most rapidly accumulating environments such as subaqueous prograding delta fronts. Therefore, we compare our results in the wider spectrum of river benthic sediments (see Tables S2 and S3) selecting those reported in the literature as MPs/kg dry weight. MP average concentration found in the Po prodelta sediments (139.7 ± 80 MPs/kg d.w.) are one order of magnitude lower than those reported for the Ebro River (2052 ± 746 MPs/kg, Simon-Sánchez et al., 2019) though the Authors worked on a wider range of classes including the >3000 μm. The same applies to values reported for the Red River Estuary (2188 ± 1499 MPs/kg, Da Le et al., 2023), one of most polluted Asiatic rivers, for similar classes 1.3–500 μm (Martin et al., 2022; Phuong et al., 2022). On the other hand, the MP concentrations in the Po prodelta are of the same order of magnitude as Bohay Bay (234 ± 89 MPs/kg, Wu et al., 2019) and the Miri Estuary (250 ± 30 MPs/kg, Liong et al., 2021) even if in both works Authors considered a wider spectrum of classes (0.003–5000 μm). Finally, the MPs concentration of the Po prodelta is one order of magnitude higher than those found in the Yangtze Estuary (35 MPs/kg, 75–5000 μm, Li et al., 2020), the Karnaphuli River (39.2 ± 14 MPs/kg, 125–5000 μm, Rakib et al., 2022), the Chao Phraya River (39 ± 14 MPs/kg, 0.05–5000 μm, Ta and

Table 4
Comparison of literature data regarding the concentration of MPs in the Norther Adriatic Sea.

Compartment	Period of the sampling	Site	Max concentration	Min concentration	Average concentration	Comments	Reference
Superficial sediments (0–5 cm)	–	Lagoon of Venice, Italy	2175 MPs/kg d.w	672 MPs/kg d.w	1445.2 (±458.4) MPs/kg d.w	Prevalence of non-fibers (90 %); size 30–500 μm (93 %) Most abundant polymers PE (48.4 %) and PP (34.1 %); colors blue and red	Vianello et al., 2013
	June 2016	North Adriatic Sea	23.30 (±45.43) MPs/kg d.w	2.92 (±4.86) MPs/kg d.w	–	Prevalence of non-fibers (95 %); size 1–5 mm; polymers PE (34.3 %), PS (52.16 %) and PP (9.5 %)	Piehl et al., 2019
	June 2016	Po River/outer Delta/North Adriatic Sea	78.8 MPs/kg d.w	0.5 MPs/kg d.w	19.58 MPs/kg d.w	Size 1–5 mm; polymers PE (40.6 %), PS (41.74 %) and PP (13.06 %)	Atwood et al., 2019
Seabed	Fall 2014	Northern and Central Adriatic Sea	>875 items/km^2	0 items/km^2	913 ± 80 items/km^2 and 82 ± 34 kg/km^2 with plastic dominant among marine litters (80 % in terms of numbers and 62 % in terms of weight)	Depth-stratified (0–30 m, 31–50 m: 51–100 m) Plastic mainly represented by bags (25 %, 24 % and 44 %), sheets from packaging (23 %, 36 % and 19 %) and mussel nets (24 %, 9 % and 4 %)	Pasquini et al., 2016
Water column	June 2016	Po River/outer Delta/North Adriatic Sea	84 MPs/m^3	1 MP/m^3	–	Size 1–5 mm	Atwood et al., 2019
	2019 (from January to December)		3.47 MPs/kg d.w	0.29 (±0.01) MPs/kg d.w	–	Prevalence of non-fibers (69.7 %); size < 5 mm (%); polymers PE (40.5 %), PS (25.7 %) and PP (27.5 %); colors white (31,8 %), transparent (43,6 %) and colored (25,4 %)	Munari et al., 2021

Babel, 2020), the Cowichan-Koksilah Estuary (14.7 MPs/kg, 0.3–5000 μm, Alava et al., 2021), and even three orders of magnitude higher than those reported for the first 30 cm of sediment of the Great Bay Estuary (0.116 MPs/kg, class 5–1785 μm, Cheng et al., 2021). Albeit, the comparison of the different studies is difficult due to the different sampling, extraction/purification, identification methods, and concentration units chosen by the different researchers to characterize the occurrence of MPs in the natural environment. This first assessment of the MP occurrence in the Po river prodelta suggests that such depositional systems should be considered a pool for MP sequestration.

4.2. MPs distribution inside a subaqueous prodelta

River mouths are the dynamic dispersal sites of riverine sediments (Coleman and Wright, 1975). Sediment flows across river mouths spatially segregate their sediment load according to density, shape, and size of the grains (Choux and Druitt, 2002; Hodson and Alexander, 2010; Luthi, 1981; Mériaux and Kurz-Besson, 2017; Pyles et al., 2013); sediment laden flows carry, entrain or deposit grains depending on their type and grain-support mechanisms, which vary spatially and temporally (Baas et al., 2011; Fildani et al., 2018; Kane et al., 2017; Stevenson et al., 2014; Talling et al., 2012). Despite the recognition of deltas as extremely dynamic environments, we have a limited ability to predict MPs concentrations in distinctive sectors of a delta and particularly so for their sub-environments in subaqueous prodeltas. The time-lapse bathymetry acquired off the Po River mouth (Fig. 1) reveals a complex geomorphology of the prodelta with the presence of erosional features and mobile bedforms that recorded disproportional concentration in MPs. The active lobe and its distal reaches exhibit the minimum and maximum concentration of MPs, respectively (Fig. 12). The absence of MPs in the coarse-grained lobe can be explained by the dilution of MPs within rapidly deposited clastic sediment (depocenter of ca. 1.3 Mm^3 of clastic sediment) or by their bypass further offshore. The maximum MPs concentration of 625 MPs/kg d.w. has been found in the distal reaches of the active lobe (sample Picnic 7) where fine-grained sediment is deposited by waning flows in a river-freshened waters that promotes flocculation as river flow energy dissipates (Boldrin et al., 1988; Fox et al., 2004), and where wave-supported gravity flow transport is negligible (Friedrichs and Scully, 2007; Traykovski et al., 2007). Where sediment flows decrease in energy both spatially and temporally, lower density or finer grains can be transported further offshore (e.g., Zavala et al., 2012; McArthur et al., 2017; Paull et al., 2018), as documented for low-density particulate organic carbon offshore the Po River mouth (Tesi et al., 2013). This suggests that MPs bypassed the proximal area (i.e. the active lobe) and have been transported in suspension into the distal reaches of the lobe (Fig. 12). This process of water elutriation (Walling and Woodward, 1993) would hinder the upward migration of larger grains within the sediment flow due to mechanical sorting mechanisms (e.g. grain-to-grain interactions) that usually result in a more homogeneous distribution of the microplastic within a lithosome (e.g. Möbius et al., 2001). In prodeltaic settings, the sinking of microplastics would be facilitated by the mixing of fresh and salty water (Simon-Sánchez et al., 2019). In the case of the Po River prodelta, these sites correspond also to the sector where sediments show the highest water content (Fig. 10 and Table 1), suggesting that sediment porosity increases intergranular accommodation and thus the possibility in trapping MPs among sedimentary particles.

Distal lobes are environments with high biodiversity of burrowing organisms (Crimes, 1977; Heard and Pickering, 2007; Tunis and Uchman, 1996; Uchman, 2004; Wheatcroft et al., 2006), such as the edible gray shrimp of the Po Delta. Consequently, microplastic fragments in these environments have a higher potential to readily enter into the marine food chain and eventually the fish market, with direct impact on human health (Ivar do Sul and Costa, 2007; Graham and Thompson, 2009; Lusher, 2015; Rochman et al., 2015; Li et al., 2016; Taylor et al., 2016; United Nations Environment Programme [UNEP], 2016; Courtene-Jones et al., 2017; Fernandez-Arcaya et al., 2017; Kedzierski et al., 2019; Näkki et al., 2017; Nelms et al., 2019; Astner et al., 2020). Macroinvertebrates such as Bivalvia and Gastropoda, which as non-selective feeders are more likely to ingest microplastic particles compared to predators and selective feeders (Scherer et al., 2020), also inhabit prodelta environments and are primary target species for bottom trawl fishing, which is relevant for the local economy.

Samples Picnic 5 and 6 come from other sites with relevant concentration of MPs (Table 2 and Fig. 10). These samples were retrieved in transverse bars that migrate dominantly southwards in response to the West Adriatic Coastal Current (Sherwood et al., 2004; Bosman et al., 2020; Trincardi et al., 2020) suggesting a lateral deviation of MPs compared to the river mouth once delivered at Sea (Fig. 12). In fact, under ordinary conditions, the freshwater plume flows for tens/hundreds of kilometers from the mouth area along the western Adriatic coast (Gacic et al., 1999; Wang and Pinardi, 2002; Eusebi Borzelli and Carniel, 2023). Particles suspended in the freshwater plume are thus dispersed along its path. The maximum concentration of MPs and cellulosic fibers in the down-current side of the delta would therefore strengthen the hypothesis that these could be directly correlated to the dispersion of the plume mainly oriented toward the southern sectors (Gacic et al., 1999). Interestingly, these active bedforms are

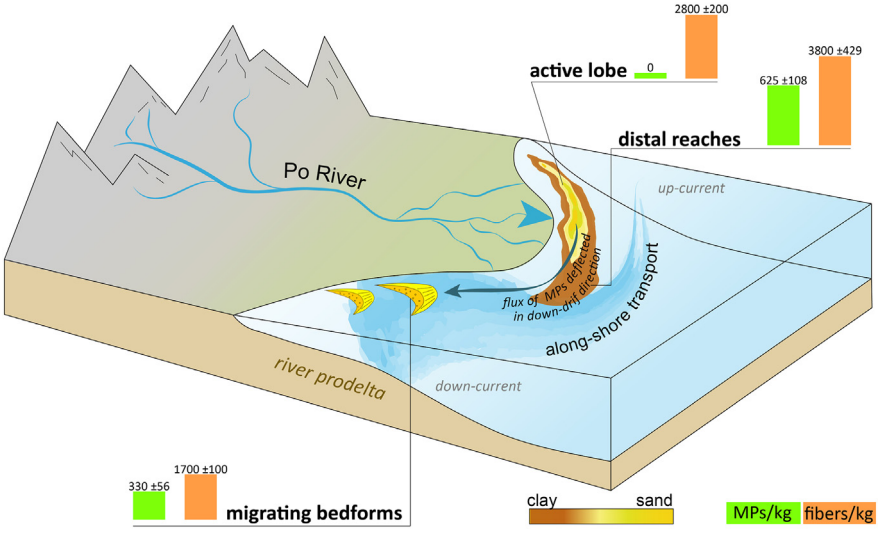

Fig. 12. Sketch of the subaqueous Po River delta summarizing the lateral heterogeneity of MPs and fibers concentrations as a result of the interplay between river flood and the marine regime. Once delivered at Sea, MPs and fibers tend to bypass the proximal sector (active lobe) and to be transported deflected in a down-drift direction.

located on the down-current side of the delta mouth (Fig. 1), where small gyres characterized by a low current velocity (ca. 5 cm/s; Maicu et al., 2018) concur in a focused deposition of MPs. This observation agrees with earlier documentation in the deep-sea environment (Kane et al., 2020) that showed localized deposition of MPs in sectors of gyres characterized by low-velocity current (shear stress < ~0.04 N m − 2). However, these bedforms are also sites of bottom trawl fisheries (Fig. 13) with lost or damaged fishing gears and nets that can act as local microplastic sources as suggested elsewhere (GESAMP, 2016; Martin et al., 2017; Buhl-Mortensen and Buhl-Mortensen, 2018; Coughlan et al., 2021).

Finally, MPs are usually found also in the coarse-grained basal portion of river flood deposits. The capacity of the denser basal layers of river flows to carry material with different size, shape and density is well-known (e.g., Paull et al., 2018), allowing low-density plastic waste to be transported as traction load (Kane and Clare, 2019; Zhong and Peng, 2021). This suggests that MPs can be stored in the basal layer of the Po River active lobe that we could not reach with the grab sampling. If this is the case, we are underestimating the total number of MPs sequestered in this coastal system.

In summary, our findings suggest that the Po prodelta is a heterogeneous depositional system characterized by a complex morphology related to a strong interplay between the river and the marine regime that in turn promoted lateral heterogeneity in sediment distribution and a patchy accumulation of MPs (Fig. 12). This suggests caution in the environmental management of these delicate ecosystems as hot spot of seabed microplastic accumulation can be created inside prodelta area which are crucial as biodiversity hotspots are also likely to be microplastic hotspots, as already envisaged for other marine areas (Kane et al., 2020).

4.3. High prevalence of cellulosic fibers

Regarding fiber abundance in the Po River prodelta, our results showed a predominance of cellulose fibers, exceeding the number of MPs in all the samples (Table 4). This agrees with other studies showing a prevalence of fibers as microdebris in the environment e.g. in the subsurface oceanic water (Suaria et al., 2020), in the seafloor sediments (Sanchez-Vidal et al., 2018; Filgueiras et al., 2021; Cannas et al., 2017; Graca et al., 2017), in the sea ice (Chubarenko et al., 2020) and even in the Adriatic food webs (Avio et al., 2020). A recent study by Suaria et al. (2020) highlighted that most of the fibers detected in seawater samples are composed of dyed cellulose suggesting natural fibers prevailing on synthetic fibers (62 %; Suaria et al., 2020). In a recent work Stanton et al. (2019) document a dominance of natural fibers in upstream reaches of the River Trent, UK (97.7 %), as well as into the shallow atmosphere of its catchment (87.3 %; Stanton et al., 2019). As expected for MPs (Wright and Kelly, 2017; Ferrero et al., 2022), fibers could be injected into the air. Moreover, textile microfibers of natural (74 % cotton, 7 % wool) and non-synthetic origins (8 %) resulted more abundant (~89 %) even in Adriatic fish and invertebrates, occurring with higher frequencies with respect to microplastics (Avio et al., 2020). Similarly, Remy et al. (2015) highlighted that the fibers found in the stomach of macroinvertebrates were mainly cellulose.

Only recently, scientists started to pay attention to the presence of cellulosic fibers in the environment as possible contaminants (Lott et al., 2022). Previously, cellulosic fibers were not included in the "microplastic" category. However, some cellulose fibers display hints on an anthropogenic origin i.e. size (10–30 um diameter), dyed color and curly shape, that are related to a possible synthetic process (Suaria et al., 2020). Furthermore, μFTIR microspectroscopy is the most currently employed analytical technique for the detection and chemical characterization of microfibers in environmental matrices and this technique is not capable of discriminating between cellulose fibers (e.g. cotton, linen) and rayon/viscose ones (Weideman et al., 2020).

In this scenario, Weideman et al. (2020) carried out a wide investigation in the Orange-Vaal River system, South Africa, where microfibers accounted for 99 % of the detected items (Weideman et al., 2020). Microfibers and microplastics were particularly abundant in the lower river reaches, while larger plastic items were less abundant (Weideman et al., 2020). Looking at the potential sources of fibers in the environment, the contribution of textiles washing is widely considered as the major: Napper and Thompson (2016), demonstrated that an average 6 kg wash load of acrylic fabric could release 700,000 fibers, making the laundering in washing machines an important pathway to aquatic habitats (Napper and Thompson, 2016). Considering the population of North Italy is around 12 million inhabitants (ISTAT, dati index, 2020) high amounts of fibers are expected to reach the Po river through the sewage system. Our results clearly indicated the dominance of cellulosic fibers (94 %) over synthetic polymers in benthic sediment of river prodelta, being one order of magnitude higher than the concentration retrieved for plastic particles (average of 2262.5 ± 338 fibers/kg d.w.). Moreover, with respect to microplastics, cellulosic fibers have been found in all the benthic sediment samples of river prodelta, sustaining the hypothesis that fibers are less stratified and more homogeneously distributed compared to plastic particles. Similar hypothesis was experimentally documented by flume tank experiments (Kane and Clare, 2019; Pohl et al., 2022). We found the highest concentrations of fibers, as for the MPs (see Section 4.2), in sample Picnic 7 (3800 fiber/kg d.w.) where it is expected that fibers are dragged downward by flocculating muddy grains as river flow energy dissipated. Recent sedimentological studies have shown that flocculating mud grains can achieve medium sand size having similar transport fate (e.g. Macquaker et al., 2010; Schieber, 2011). Another site with important concentration is Picnic 8

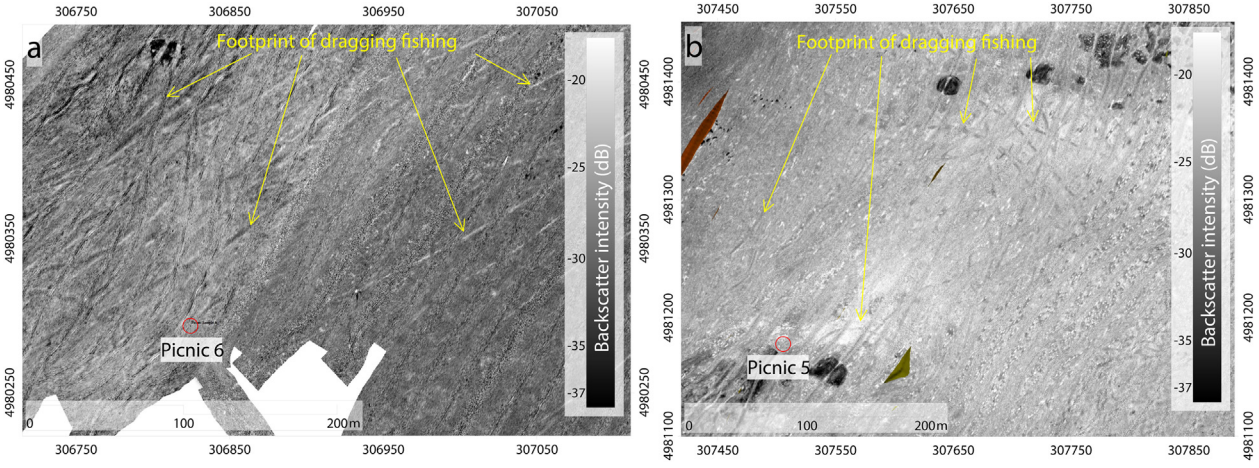

Fig. 13. Backscatter data from hull-mounted multibeam bathymetric data showing the presence of trawl marks in the prodelta sector interested by the presence of sandy migrating bedforms.

(3400 fiber/kg d.w.). Here, fibers have been trapped with settling sand grains during the formation of the delta bar and do not suffer from the erosion by wave action in this shallower sector (Bosman et al., 2019; Trincardi et al., 2020). Noteworthy, the fiber size distribution observed in four samples (Picninc 5,6,8, and 11) displayed a power-law size distribution with a scaling exponent of 1 that is consistent with a fragmentation along one dimension (Cózar et al., 2014). This strict relation of the fiber abundance with the size class indicates the absence of any size dependent selection mechanism operating during the fiber's deposition process in the Po delta transitional environment. This can be the result of a rapid deposition and burial faced by sediment in the proximal prodelta compared to sediment undergoing longer transport time (and traveling distance) for example in the outer shelf (e.g., Saliu et al., 2022), canyons and deep-sea contourites (e.g. Kane et al., 2020), for which the occurrence of particle selection during the offshore transport can be expected. A significant difference in size was highlighted only for cellulose fibers <0.5 mm between active lobe and prodelta migrating bedforms ($p < 0.005$, Fig. 9), suggesting that particle selection likely operate along the river mouth-sea transect that follows the southward along-shore sediment redistribution. This evidence implies that the transport of fibers occurs parallel to the coast as the oceanographic regime dominates on river processes, determining fiber pools skewed in respect to the river entry point.

Finally, considering the reported average density for cellulose textile (1.54–1.63 g cm^{-3}), which are higher than the most common polymers found in the marine environment (polyolefin, 0.90 g cm^{-3}), cellulose fibers, even if not surely related to anthropogenic pollution, may be used as a proxy of the deposition processes and discussed together with MPs.

5. Conclusion

Time-lapse bathymetry and benthic sediment sampling allowed us to draw a relationship between the complex geomorphology of the Po prodelta and the patchy sequestration of MP and pollutants-related particles. Our results show that the distribution of microplastics in these environments is two orders of magnitude higher than most benthic river sediments currently reported in the literature, thus prodelta lithosome represent a pool of MPs accumulation. Furthermore, high spatial heterogeneity of microplastic accumulation in these environments is mainly related to the type of river flood transport and to the dominant oceanographic regime at the river mouth. Once delivered at sea, MPs and fibers tend to be transported laterally with respect to the river mouth and to concentrate in the finer-grained distal deposits of the active lobe and particularly in the down current side of the river mouth, in sectors where the shear stress is low. In the case of the Po prodelta, these sectors have significant economic value because they correspond to high biodiversity of the scavenging macrofauna and are therefore preferential sites for bottom trawling, posing a problem on contamination of the food chain and potential threat to human health. Overall, natural fibers are predominant in all geomorphological sectors and overwhelmed synthetic polymers by two orders of magnitude. This study highlighted the importance of morphodynamic information in guiding the monitoring and sampling of microplastic along subaqueous coastal sectors that can represent significant albeit underestimated hotspots in terms of MPs and associated pollutants sequestration.

Supplementary data to this article can be found online at https://doi.org/10.1016/j.scitotenv.2023.164908.

CRediT authorship contribution statement

Pellegrini, C. geophysical data acquisition and interpretation, wrote paper, visualization, conceptualization; **Saliu, F.** phthalate and microplastic analyses and writing; **Bosman, A.** geophysical data acquisition and processing, visualization review & editing; **Sammartino, I.** provenance analyses, writing; **Raguso C.** microplastic analyses; **Mercorella, A.** geophysical data acquisition and processing; **Galvez, D.S.** geophysical data acquisition and processing, review & editing; **Petrizzo, A.** geophysical data acquisition and processing, review; **Madricardo, F.** geophysical data acquisition review; **Lasagni, M.** fthalate and microplastic analyses; **Clemenza, M.** fthalate and microplastic analyses; **Trincardi, F.** review & editing, **Rovere, M.** review & editing, Funding acquisition.

Data availability

Data will be made available on request.

Declaration of competing interest

Claudio Pellegrini reports financial support was provided by European Union. Claudio Pellegrini reports a relationship with National Research Council of Italy that includes: board membership. Nothing to declare.

Acknowledgments

This project has received funding from the European Union's Horizon 2020 Research and Innovation Programme under grant agreement No 101004221, and from the Italian Ministry of Research under the PRIN PASS project “The Po-Adriatic Source-to-Sink system: from modern sedimentary processes to millennial-scale stratigraphic architecture”, contract 2017ASZAKJ_001. Editor Damià Barceló and two anonymous Reviewers are thanked for insightful comments that improved the paper. The authors want to thank Arpae-SIMC for managing and providing the offshore wave data of the Nausicaa buoy. We thank Giulia Giorgetti and Alina Polonia (CNR-ISMAR) for the grain size analyses.

References

Alava, J.J., Kazmiruk, T.N., Douglas, T., Schuerholz, G., Heath, B., Flemming, S.A., Bendell, L., Drever, M.C., 2021. Occurrence and size distribution of microplastics in mudflat sediments of the Cowichan-Koksilah Estuary, Canada: a baseline for plastic particles contamination in an anthropogenic-influenced estuary. Mar. Pollut. Bull. 173, 113033. https://doi.org/10.1016/j.marpolbul.2021.113033.

Amorosi, A., Sammartino, I., Dinelli, E., Campo, B., Guercia, T., Trincardi, F., Pellegrini, C., 2022. Provenance and sediment dispersal in the Po-Adriatic source-to-sink system unraveled by bulk-sediment geochemistry and its linkage to catchment geology. Earth-Sci. Rev. 234, 104202. https://doi.org/10.1016/j.earscirev.2022.104202.

Anthony, E.J., Marriner, N., Morhange, C., 2014. Human influence and the changing geomorphology of Mediterranean deltas and coasts over the last 6000 years: from progradation to destruction phase? Earth Sci. Rev. 139, 336–361. https://doi.org/10.1016/j.earscirev.2014.10.003.

Artegiani, A., Paschini, E., Russo, A., Bregant, D., Raicich, F., Pinardi, N., 1997. The Adriatic Sea general circulation. Part II: baroclinic circulation structure. J. Phys. Oceanogr. 27, 1515–1532. https://doi.org/10.1175/1520-0485(1997)027<1515:TASGCP>2.0.CO;2.

Astner, A.F., Hayes, D.G., Pingali, S.V., O'Neill, H.M., Littrell, K.C., Evans, B.R., Urban, V.S., 2020. Effects of soil particles and convective transport on dispersion and aggregation of nanoplastics via small-angle neutron scattering (SANS) and ultra SANS (USANS). PLoS One 15 (7), e0235893. https://doi.org/10.1371/journal.pone.0235893.

Atwood, E.C., Falcieri, F.M., Piehl, S., Bochow, M., Matthies, M., Franke, J., Carniel, S., Sclavo, M., Laforsch, C., Siegert, F., 2019. Coastal accumulation of microplastic particles emitted from the Po River, Northern Italy: comparing remote sensing and hydrodynamic modelling with in situ sample collections. Mar. Pollut. Bull. 138, 561–574.

Avio, C.G., Pittura, L., d'Errico, G., Abel, S., Amorello, S., Marino, G., Gorbi, S., Regoli, F., 2020. Distribution and characterization of microplastic particles and textile microfibers in Adriatic food webs: general insights for biomonitoring strategies. Environ. Pollut. 2020 (258), 113766. https://doi.org/10.1016/j.envpol.2019.113766.

Baas, J.H., Best, J.L., Peakall, J., 2011. Depositional processes, bedform development and hybrid bed formation in rapidly decelerated cohesive (mud-sand) sediment flows: Bedforms in decelerated cohesive flows. Sedimentology 58, 1953–1987. https://doi.org/10.1111/j.1365-3091.2011.01247.x.

Baudena, A., Ser-Giacomi, E., Jalón-Rojas, I., Galgani, F., Pedrotti, M.L., 2022. The streaming of plastic in the Mediterranean Sea. Nat. Commun. 13 (1), 1–9.

Bianchi, T.S., Cui, X., Blair, N.E., Burdige, D.J., Eglinton, T.I., Galy, V., 2018. Centers of organic carbon burial and oxidation at the land-ocean interface. Org. Geochem. 115, 138–155. https://doi.org/10.1016/j.orggeochem.2017.09.008.

Blott, S.J., Pye, K., 2001. GRADISTAT: a grain size distribution and statistics package for the analysis of unconsolidated sediments. Earth Surf. Process. Landf. 26, 1237–1248. https://doi.org/10.1002/esp.261.

Blum, M.D., Roberts, H.H., 2009. Drowning of the Mississippi Delta due to insufficient sediment supply and global sea-level rise. Nat. Geosci. 2, 488–491. https://doi.org/10.1038/ngeo553.

Boldrin, A., Bortoluzzi, G., Frascari, F., Guerzoni, S., Rabitti, S., 1988. Recent deposits and suspended sediments off the Po della Pila (Po River, main mouth), Italy. Mar. Geol. 79, 159–170. https://doi.org/10.1016/0025-3227(88)90037-0.

Boldrin, A., Langone, L., Miserocchi, S., Turchetto, M., Acri, F., 2005. Po River plume on the Adriatic continental shelf: dispersion and sedimentation of dissolved and suspended matter during different river discharge rates. Mar. Geol. 222–223, 135–158. https://doi.org/10.1016/j.margeo.2005.06.010.

Bosman, A., Casalbore, D., Anzidei, M., Muccini, F., Carmisciano, C., Francesco Latino, C., 2015. The first ultra-high resolution digital terrain model of the shallow-water sector around Lipari Island (Aeolian Islands, Italy). Ann. Geophys. 58, 2.. http://hdl.handle.net/2122/9478.

Bosman, A., Romagnoli, C., Madricardo, F., Correggiari, A., Remia, A., Zubalich, R., Fogarin, S., Kruss, A., Trincardi, F., 2020. Short-term evolution of Po della Pila delta lobe from time lapse high-resolution multibeam bathymetry (2013–2016). Estuar. Coast. Shelf Sci. 233, 106533. https://doi.org/10.1016/j.ecss.2019.106533.

Boucher, J., Bilard, G., 2020. The Mediterranean: Mare Plasticum. IUCN (International Union for Conservation of Nature), Gland, Switzerland, p. 62.

Buhl-Mortensen, P., Buhl-Mortensen, L., 2018. Impacts of bottom trawling and litter on the seabed in Norwegian waters. Front. Mar. Sci. 5, 42. https://doi.org/10.3389/fmars.2018.00042.

Canals, M., Pham, C.K., Bergmann, M., Gutow, L., Hanke, G., Van Sebille, E., ... Giorgetti, A., 2021. The quest for seafloor macrolitter: a critical review of background knowledge, current methods and future prospects. Environ. Res. Lett. 16 (2), 023001.

Cannas, S., Fastelli, P., Guerranti, C., Renzi, M., 2017. Plastic litter in sediments from the coasts of South Tuscany (Tyrrhenian Sea). Mar. Pollut. Bull. 119, 372–375. https://doi.org/10.1016/j.marpolbul.2017.04.008.

Cheng, M.L.H., Lippmann, T.C., Dijkstra, J.A., Bradt, G., Cook, S., Choi, J.-G., Brown, B.L., 2021. A baseline for microplastic particle occurrence and distribution in Great Bay Estuary. Mar. Pollut. Bull. 170, 112653. https://doi.org/10.1016/j.marpolbul.2021.112653.

Choux, C.M., Druitt, T.H., 2002. Analogue study of particle segregation in pyroclastic density currents, with implications for the emplacement mechanisms of large ignimbrites. Sedimentology 49, 907–928. https://doi.org/10.1046/j.1365-3091.2002.00481.x.

Chubarenko, I., Efimova, I., Bagaeva, M., Bagaev, A., Isachenko, I., 2020. On mechanical fragmentation of single-use plastics in the sea swash zone with different types of bottom sediments: insights from laboratory experiments. Mar. Pollut. Bull. 150, 110726. https://doi.org/10.1016/j.marpolbul.2019.110726.

Coleman, J.M., Wright, L.D., 1975. Modern River Deltas: Variability of Processes and Sand Bodies.

Costa, M.F., Silva-Cavalcanti, J.S., Barbosa, C.C., Portugal, J.L., Barletta, M., 2011. Plastics buried in the inter-tidal plain of a tropical estuarine ecosystem. J. Coast. Res., 339–343.. https://www.jstor.org/stable/26482189.

Coughlan, M., Guerrini, M., Creane, S., O'Shea, M., Ward, S.L., Van Landeghem, K.J., Doherty, P., 2021. A new seabed mobility index for the Irish Sea: modelling seabed shear stress and classifying sediment mobilisation to help predict erosion, deposition, and sediment distribution. Cont. Shelf Res. 229, 104574. https://doi.org/10.1016/j.csr.2021.104574.

Courtene-Jones, W., Quinn, B., Gary, S.F., Mogg, A.O., Narayanaswamy, B.E., 2017. Microplastic pollution identified in deep-sea water and ingested by benthic invertebrates in the Rockall Trough, North Atlantic Ocean. Environ. Pollut. 231, 271–280. https://doi.org/10.1016/j.envpol.2017.08.026.

Cózar, A., Echevarría, F., González-Gordillo, J.I., Irigoien, X., Úbeda, B., Hernández-León, S., Palma, Á.T., Navarro, S., García-de-Lomas, J., Ruiz, A., Fernández-de-Puelles, M.L., Duarte, C.M., 2014. Plastic debris in the open ocean. Proc. Natl. Acad. Sci. 111, 10239–10244. https://doi.org/10.1073/pnas.1314705111.

Crimes, T.P., 1977. Trace fossils of an Eocene deep-sea fan, northern Spain. In: Crimes, P.T., Harper, J.C. (Eds.), Trace Fossils 2. 9. Geol Soc Spec Publ, pp. 71–90.

Da Le, N., Hoang, T.T.H., Duong, T.T., Phuong, N.N., Le, P.T., Nguyen, T.D., Phung, T.X.B., Le, T.M.H., Le, T.L., Vu, T.H., Le Le, T.P.Q., 2023. Microplastics in the surface sediment of the main Red River Estuary. Vietnam J. Earth Sci. 45 (1), 19–32. https://doi.org/10.15625/2615-9783/17486.

Dai, Z., Liu, J.T., Wei, W., Chen, J., 2014. Detection of the Three Gorges Dam influence on the Changjiang (Yangtze River) submerged delta. Sci. Rep. 4, 6600. https://doi.org/10.1038/srep06600.

Duan, Z., Zhao, S., Zhao, L., Duan, X., Xie, S., Zhang, H., Liu, Y., Peng, Y., Liu, C., Wang, L., 2020. Microplastics in Yellow River Delta wetland: occurrence, characteristics, human influences, and marker. Environ. Pollut. 258, 113232. https://doi.org/10.1016/j.envpol.2019.113232.

Duncan, E.M., Arrowsmith, J., Bain, C., Broderick, A.C., Lee, J., Metcalfe, K., Godley, B.J., 2018. The true depth of the Mediterranean plastic problem: extreme microplastic pollution on marine turtle nesting beaches in Cyprus. Mar. Pollut. Bull. 136, 334–340.

Eusebi Borzelli, G.L., Carniel, S., 2023. A reconciling vision of the Adriatic-Ionian bimodal oscillating system. Sci. Rep. 13 (1), 2334. https://doi.org/10.1038/s41598-023-29162.

Falcieri, F.M., Benetazzo, A., Sclavo, M., Russo, A., Carniel, S., 2014. Po River plume pattern variability investigated from model data. Cont. Shelf Res. 87, 84–95. https://doi.org/10.1016/j.csr.2013.11.001.

Fernandez-Arcaya, U., Ramirez-Llodra, E., Aguzzi, J., Allcock, A.L., Davies, J.S., Dissanayake, A., Harris, P., Howell, K., Huvenne, V.A.I., Macmillan-Lawler, M., Martín, J., Menot, L., Nizinski, M., Puig, P., Rowden, A.A., Sanchez, F., Van den Beld, I.M.J., 2017. Ecological role of submarine canyons and need for canyon conservation: a review. Front. Mar. Sci. 4. https://doi.org/10.3389/fmars.2017.00005.

Ferrero, L., Scibetta, L., Markuszewski, P., Mazurkiewicz, M., Drozdowska, V., Makuch, P., Jutrzenka-Trzebiatowska, P., Zaleska-Medynska, A., Andò, S., Saliu, F., Nilsson, E.D., Bolzacchini, E., 2022. Airborne and marine microplastics from an oceanographic survey at the Baltic Sea: an emerging role of air-sea interaction? Sci. Total Environ. 824, 153709. https://doi.org/10.1016/j.scitotenv.2022.153709.

Fildani, A., Hessler, A.M., Mason, C.C., McKay, M.P., Stockli, D.F., 2018. Late Pleistocene glacial transitions in North America altered major river drainages, as revealed by deep-sea sediment. Sci. Rep. 8, 13839. https://doi.org/10.1038/s41598-018-32268-7.

Filgueiras, A.V., Gago, J., García, I., León, V.M., Viñas, L., 2021. Plackett Burman design for microplastics quantification in marine sediments. Mar. Pollut. Bull. 162, 111841. https://doi.org/10.1016/j.marpolbul.2020.111841.

Fox, J.M., Hill, P.S., Milligan, T.G., Boldrin, A., 2004. Flocculation and sedimentation on the Po River Delta. Mar. Geol. 203 (1–2), 95–107. https://doi.org/10.1016/S0025-3227(03)00332-3.

Franzini, M., Leoni, L., Saitta, M., 1972. A simple method to evaluate the matrix effects in X-Ray fluorescence analysis. X-Ray Spectrom. 1, 151–154. https://doi.org/10.1002/xrs.1300010406.

Friedrichs, C.T., Scully, M.E., 2007. Modeling deposition by wave-supported gravity flows on the Po River prodelta: from seasonal floods to prograding clinoforms. Cont. Shelf Res. 27, 322–337. https://doi.org/10.1016/j.csr.2006.11.002.

Gacic, M., Civitarese, G., Ursella, L., 1999. Spatial and seasonal variability of water and biogeochemical fluxes in the Adriatic Sea. In: Malanotte-Rizzoli, P., Eremeev, V.N. (Eds.), The Eastern Mediterranean as a Laboratory Basin for the Assessment of Contrasting Ecosystems. Kluwer Academic Publishers, pp. 335–357.

Gago, J., Booth, A.M., Tiller, R., Maes, T., Larreta, J., 2020. Microplastics pollution and regulation. Handbook of Microplastics in the Environment, pp. 1–27.

Galgani, F., 2015. Marine litter, future prospects for research. Front. Mar. Sci. 2, 87. https://doi.org/10.3389/fmars.2015.00087.

Galgani, F., Hanke, G., Werner, S.D.V.L., De Vrees, L., 2013. Marine litter within the European marine strategy framework directive. ICES J. Mar. Sci. 70 (6), 1055–1064.

Garcés-Ordóñez, O., Saldarriaga-Vélez, J.F., Espinosa-Díaz, L.F., Canals, M., Sánchez-Vidal, A., Thiel, M., 2022. A systematic review on microplastic pollution in water, sediments, and organisms from 50 coastal lagoons across the globe. Environ. Pollut. 315, 1–15 120366.

GESAMP, 2016. Sources, fate and effects of microplastics in the marine environment: part two of a global assessment. In: Kershaw, P.J., Rochman, C.M. (Eds.), (IMO/FAO/UNESCO-IOC/UNIDO/WMO/IAEA/UN/UNEP/UNDP Joint Group of Experts on the Scientific Aspects of Marine Environmental Protection). Rep. Stud. GESAMP No. 93 (220 p).

Gissi, E., Gaglio, M., Reho, M., 2014. Trade-off between carbon storage and biomass-based energy sources ecosystem services, the case study from the province of Rovigo (Italy). Ann. Bot. 4, 73–81. https://doi.org/10.4462/annbotrm-11814.

Graca, B., Szewc, K., Zakrzewska, D., Dołęga, A., Szczerbowska-Boruchowska, M., 2017. Sources and fate of microplastics in marine and beach sediments of the southern Baltic Sea—a preliminary study. ESPR 24 (8), 7650–7661. https://doi.org/10.1007/s11356-017-8419-5.

Graham, E.R., Thompson, J.T., 2009. Deposit-and suspension-feeding sea cucumbers (Echinodermata) ingest plastic fragments. J. Exp. Mar. Biol. Ecol. 368 (1), 22–29. https://doi.org/10.1016/j.jembe.2008.09.007.

Heard, T.G., Pickering, K.T., 2007. Trace fossils as diagnostic indicators of deep-marine environments, Middle Eocene Ainsa-Jaca basin, Spanish Pyrenees: trace fossils as diagnostic indicators of deep-marine environments. Sedimentology 55, 809–844. https://doi.org/10.1111/j.1365-3091.2007.00922.x.

Hodson, J.M., Alexander, J., 2010. The effects of grain-density variation on turbidity currents and some implications for the deposition of carbonate turbidites. J. Sediment. Res. 80, 515–528. https://doi.org/10.2110/jsr.2010.051.

Hood, W.G., 2010. Delta distributary dynamics in the Skagit River Delta (Washington, USA): extending, testing, and applying avulsion theory in a tidal system. Geomorphology 123, 154–164. https://doi.org/10.1016/j.geomorph.2010.07.007.

Horton, A.A., Walton, A., Spurgeon, D., Lahive, E., Svendsen, C., 2017. Microplastics in freshwater and terrestrial environments: evaluating the current understanding to identify the knowledge gapsand future research priorities. Sci. Total Environ. 586, 127–141. https://doi.org/10.1016/j.scitotenv.2017.01.190.

Hu, L., Chernick, M., Hinton, D.E., Shi, H., 2018. Microplastics in small waterbodies and tadpoles from Yangtze River Delta, China. Environ. Sci. Technol. 52, 8885–8893. https://doi.org/10.1021/acs.est.8b02279.

Hurley, R., Woodward, J., Rothwell, J.J., 2018. Microplastic contamination of river beds significantly reduced by catchment-wide flooding. Nat. Geosci. 11, 251–257. https://doi.org/10.1038/s41561-018-0080-1.

IPCC, 2021. Climate Change. The Physical Science Basis. Working Group I Contribution to the IPCC Sixth Assessment Report.

Ivar do Sul, J.A., Costa, M.F., 2007. Marine debris review for Latin America and the wider Caribbean region: from the 1970s until now, and where do we go from here? Mar. Pollut. Bull. 54, 1087–1104. https://doi.org/10.1016/j.marpolbul.2007.05.004.

Kane, I.A., Clare, M.A., 2019. Dispersion, accumulation, and the ultimate fate of microplastics in deep-marine environments: a review and future directions. Front. Earth Sci. 7, 80. https://doi.org/10.3389/feart.2019.00080.

Kane, I.A., Fildani, A., 2021. Anthropogenic pollution in deep-marine sedimentary systems—a geological perspective on the plastic problem. Geology 49 (5), 607–608. https://doi.org/10.1130/focus052021.1.

Kane, I.A., Pontén, A.S., Vangdal, B., Eggenhuisen, J.T., Hodgson, D.M., Spychala, Y.T., 2017. The stratigraphic record and processes of turbidity current transformation across deep-marine lobes. Sedimentology 64 (5), 1236–1273. https://doi.org/10.1111/sed.12346.

Kane, I.A., Clare, M.A., Miramontes, E., Wogelius, R., Rothwell, J.J., Garreau, P., Pohl, F., 2020. Seafloor microplastic hotspots controlled by deep-sea circulation. Science 368, 1140–1145. https://doi.org/10.1126/science.aba5899.

Kedzierski, M., Falcou-Préfol, M., Kerros, M.E., Henry, M., Pedrotti, M.L., Bruzaud, S., 2019. A machine learning algorithm for high throughput identification of μFTIR spectra: application on microplastics collected in the Mediterranean Sea. Chemosphere 234, 242–251. https://doi.org/10.1016/j.chemosphere.2019.05.113.

Kelleher, L., Schneidewind, U., Krause, S., Haverson, L., Allen, S., Allen, D., Kukkola, A., Murray-Hudson, M., Maselli, V., Franchi, F., 2023. Microplastic accumulation in endorheic river basins–the example of the Okavango Panhandle (Botswana). Sci. Total Environ. 874, 162452. https://doi.org/10.1016/j.scitotenv.2023.162452.

Kurki-Fox, J.J., Doll, B.A., Monteleone, B., West, K., Putnam, G., Kelleher, L., Krause, S., Schneidewind, U., 2023. Microplastic distribution and characteristics across a large

river basin: insights from the Neuse River in North Carolina, USA. Sci. Total Environ. 878, 162940. https://doi.org/10.1016/j.scitotenv.2023.162940.
Lebreton, L.C.M., van der Zwet, J., Damsteeg, J.-W., Slat, B., Andrady, A., Reisser, J., 2017. River plastic emissions to the world's oceans. Nat. Commun. 8, 15611. https://doi.org/10.1038/ncomms15611.
Lebreton, L., Egger, M., Slat, B., 2019. A global mass budget for positively buoyant macroplastic debris in the ocean. Sci. Rep. 9, 12922. https://doi.org/10.1038/s41598-019-49413-5.
Leoni, L., Saitta, M., 1976. Determination of yttrium and niobium on standard silicate rocks by X-ray fluorescence analyses. X-Ray Spectrom. 5, 29–30. https://doi.org/10.1002/xrs.1300050107.
Leoni, L., Menichini, M., Saitta, M., 1982. Determination of S, Cl and F in silicate rocks by X-ray fluorescence analyses. X-Ray Spectrom. 11, 156–158. https://doi.org/10.1002/xrs.1300110404.
Leslie, H.A., Brandsma, S.H., Van Velzen, M.J.M., Vethaak, A.D., 2017. Microplastics en route: field measurements in the Dutch river delta and Amsterdam canals, wastewater treatment plants, North Sea sediments and biota. Environ. Int. 101, 133–142. https://doi.org/10.1016/j.envint.2017.01.018.
Li, W.C., Tse, H.F., Fok, L., 2016. Plastic waste in the marine environment: a review of sources, occurrence and effects. Sci. Total Environ. 566, 333–349. https://doi.org/10.1016/j.scitotenv.2016.05.084.
Li, Y., Lu, Z., Zheng, H., Wang, J., Chen, C., 2020. Microplastics in surface water and sediments of Chongming Island in the Yangtze Estuary, China. Environ. Sci. Eur. 32, 15. https://doi.org/10.1186/s12302-020-0297-7.
Liong, R.M.Y., Hadibarata, T., Yuniarto, A., Tang, K.H.D., Khamidun, M.H., 2021. Microplastic occurrence in the water and sediment of Miri River Estuary, Borneo Island. Water Air Soil Pollut. 232, 342. https://doi.org/10.1007/s11270-021-05297-8.
Liubartseva, S., Coppini, G., Lecci, R., Creti, S., 2016. Regional approach to modeling the transport of floating plastic debris in the Adriatic Sea. Mar. Pollut. Bull. 103, 115–127. https://doi.org/10.1016/j.marpolbul.2015.12.031.
Lott, C., Eich, A., Weber, M., 2022. Degradation of fibrous microplastics in the marine environment. Polluting Textiles. Routledge, pp. 185–213.
Lusher, A., 2015. Microplastics in the marine environment: distribution, interactions and effects. Marine Anthropogenic Litter. Springer, Cham, pp. 245–307.
Luthi, S. An, 1981. Experiments on non-channelized turbidity currents and their deposits. Mar. Geol. 40, M59–M68. https://doi.org/10.1016/0025-3227(81)90139-0.
Macquaker, J.H., Bentley, S.J., Bohacs, K.M., 2010. Wave-enhanced sediment-gravity flows and mud dispersal across continental shelves: reappraising sediment transport processes operating in ancient mudstone successions. Geology 38 (10), 947–950.
Madricardo, F., Foglini, F., Kruss, A., Ferrarin, C., Pizzeghello, N.M., Murri, C., Rossi, M., Bajo, M., Bellafiore, D., Campiani, E., Fogarin, S., Grande, V., Janowski, L., Keppel, E., Leidi, E., Lorenzetti, G., Maicu, F., Maselli, V., Mercorella, A., Montereale Gavazzi, G., Minuzzo, T., Pellegrini, C., Petrizzo, A., Prampolini, M., Remia, A., Rizzetto, F., Rovere, M., Sarretta, A., Sigovini, M., Sinapi, L., Umgiesser, G., Trincardi, F., 2017. High resolution multibeam and hydrodynamic datasets of tidal channels and inlets of the Venice Lagoon. Sci. Data 4, 170121. https://doi.org/10.1038/sdata.2017.121.
Madricardo, F., Foglini, F., Campiani, E., Grande, V., Catenacci, E., Petrizzo, A., Kruss, A., Toso, C., Trincardi, F., 2019. Assessing the human footprint on the sea-floor of coastal systems: the case of the Venice Lagoon, Italy. Sci. Rep. 9, 6615. https://doi.org/10.1038/s41598-019-43027-7.
Maicu, F., De Pascalis, F., Ferrarin, C., Umgiesser, G., 2018. Hydrodynamics of the Po River-Delta-Sea system. J. Geophys. Res. Oceans 123, 6349–6372. https://doi.org/10.1029/2017JC013601.
Martin, J., Lusher, A., Thompson, R.C., Morley, A., 2017. The deposition and accumulation of microplastics in marine sediments and bottom water from the Irish continental shelf. Sci. Rep. 7 (1), 1–9. https://doi.org/10.1038/s41598-017-11079-2.
Martin, C., Young, C.A., Valluzzi, L., Duarte, C.M., 2022. Ocean sediments as the global sink for marine micro- and mesoplastics. Limnol. Oceanogr. Lett. 7, 235–243. https://doi.org/10.1002/lol2.10257.
Maselli, V., Trincardi, F., 2013. Man made deltas. Sci. Rep. 3, 1926. https://doi.org/10.1038/srep01926.
McArthur, A.D., Gamberi, F., Kneller, B.C., Wakefield, M.I., Souza, P.A., Kuchle, J., 2017. Palynofacies classification of submarine fan depositional environments: outcrop examples from the Marnoso-Arenacea Formation, Italy. Mar. Pet. Geol. 88, 181–199. https://doi.org/10.1016/j.marpetgeo.2017.08.018.
Mériaux, C.A., Kurz-Besson, C.B., 2017. A study of gravity currents carrying polydisperse particles along a V-shaped valley. Eur. J. Mech. - BFluids 63, 52–65. https://doi.org/10.1016/j.euromechflu.2016.12.010.
Möbius, M.E., Lauderdale, B.E., Nagel, S.R., Jaeger, H.M., 2001. Size separation of granular particles. Nature 414, 270. https://doi.org/10.1038/35104697.
Munari, C., Scoponi, M., Sfriso, A.A., Sfriso, A., Aiello, J., Casoni, E., Mistri, M., 2021. Temporal variation of floatable plastic particles in the largest Italian river, the Po. Mar. Pollut. Bull. 171, 112805. https://doi.org/10.1016/j.marpolbul.2021.112805.
Näkki, P., Setälä, O., Lehtiniemi, M., 2017. Bioturbation transports secondary microplastics to deeper layers in soft marine sediments of the northern Baltic Sea. Mar. Pollut. Bull. 119 (1), 255–261. https://doi.org/10.1016/j.marpolbul.2017.03.065.
Napper, I.E., Thompson, R.C., 2016. Release of synthetic microplastic plastic fibres from domestic washing machines: effects of fabric type and washing conditions. Mar. Pollut. Bull. 112 (1–2), 39–45. https://doi.org/10.1016/j.marpolbul.2016.09.025.
Nelms, S.E., Barnett, J., Brownlow, A., Davison, N.J., Deaville, R., Galloway, T.S., Lindeque, P.K., Santillo, D., Godley, B.J., 2019. Microplastics in marine mammals stranded around the British coast: ubiquitous but transitory? Sci. Rep. 9 (1), 1–8. https://doi.org/10.1038/s41598-018-37428-3.
Nelson, B.W., 1970. Hydrography, sediment dispersal, and recent historical development of the Po River Delta, Italy. In: Morgan, J.P. (Ed.), Deltaic Sedimentation, Modern and Ancient. 15. Society of Economic Paleontologists and Mineralogists. Special Publication, Tulsa, OK, pp. 152–184.
Nguyen, T., Shih, D.-S., Chua, L., Kieu, H., Ha, L., Nguyen, L., Luu, N., Huynh, T., Duong, L., Ngo, A., Nguyen, H., Tran, C., 2022. Identifying flow Eddy currents in the river system as the riverbank scouring cause: a case study of the Mekong River. Water 14, 2418. https://doi.org/10.3390/w14152418.
Orton, G.J., Reading, H.G., 1993. Variability of deltaic processes in terms of sediment supply, with particular emphasis on grain size. Sedimentology 40, 475–512. https://doi.org/10.1111/j.1365-3091.1993.tb01347.x.
Overeem, I., Brakenridge, R.G., 2009. Dynamics and Vulnerability of Delta Systems. Vol. 35. GKSS Research Centre, LOICZ Internat. Project Office, Inst. for Coastal Research.
Paluselli, A., Aminot, Y., Galgani, F., Net, S., Sempéré, R., 2018. Occurrence of phthalate acid esters (PAEs) in the northwestern Mediterranean Sea and the Rhone River. Prog. Oceanogr. 163, 221–231. https://doi.org/10.1016/j.pocean.2017.06.002.
Pasquini, G., Ronchi, F., Strafella, P., Scarcella, G., Fortibuoni, T., 2016. Seabed litter composition, distribution and sources in the Northern and Central Adriatic Sea (Mediterranean). Waste Manag. 58, 41–51.
Paull, C.K., Talling, P.J., Maier, K.L., Parsons, D., Xu, J., Caress, D.W., Gwiazda, R., Lundsten, E.M., Anderson, K., Barry, J.P., Chaffey, M., O'Reilly, T., Rosenberger, K.J., Gales, J.A., Kieft, B., McGann, M., Simmons, S.M., McCann, M., Sumner, E.J., Clare, M.A., Cartigny, M.J., 2018. Powerful turbidity currents driven by dense basal layers. Nat. Commun. 9, 4114. https://doi.org/10.1038/s41467-018-06254-6.
Pellegrini, C., Patruno, S., Helland-Hansen, W., Steel, R.J., Trincardi, F., 2020. Clinoforms and clinothems: fundamental elements of basin infill. Basin Res. 32 (2), 187–205.
Pellegrini, C., Tesi, T., Schieber, J., Bohacs, K.M., Rovere, M., Asioli, A., Nogarotto, A., Trincardi, F., 2021. Fate of terrigenous organic carbon in muddy clinothems on continental shelves revealed by stratal geometries: insight from the Adriatic sedimentary archive. Glob. Planet. Chang. 203, 103539. https://doi.org/10.1016/j.gloplacha.2021.103539.
Phuong, N.N., Duong, T.T., Le, T.P.Q., Hoang, T.K., Ngo, H.M., Phuong, N.A., Pham, Q.T., Doan, T.O., Ho, T.C., Da Le, N., Nguyen, T.A.H., Strady, E., Fauvelle, V., Ourgaud, M., Schmidt, N., Sempere, R., 2022. Microplastics in Asian freshwater ecosystems: current knowledge and perspectives. Sci. Total Environ. 808, 151989. https://doi.org/10.1016/j.scitotenv.2021.151989.
Piehl, S., Mitterwallner, V., Atwood, E.C., Bochow, M., Laforsch, C., 2019. Abundance and distribution of large microplastics (1–5 mm) within beach sediments at the Po River Delta, Northeast Italy. Mar. Pollut. Bull. 149, 110515. https://doi.org/10.1016/j.marpolbul.2019.110515.
Pierdomenico, M., Ridente, D., Casalbore, D., Di Bella, L., Milli, S., Chiocci, F.L., 2022. Plastic burial by flash-flood deposits in a prodelta environment (Gulf of Patti, Southern Tyrrhenian Sea). Mar. Pollut. Bull. 181, 113819. https://doi.org/10.1016/j.marpolbul.2022.113819.
Pohl, A., Tytła, M., Kernert, J., Bodzek, M., 2022. Plastics-derived and heavy metals contaminants in the granulometric fractions of bottom sediments of anthropogenic water reservoir–comprehensive analysis. Desalin. Water Treat. 258, 207–222. https://doi.org/10.5004/dwt.2022.28459.
Pyles, D.R., Straub, K.M., Stammer, J.G., 2013. Spatial variations in the composition of turbidites due to hydrodynamic fractionation. Geophys. Res. Lett. 40 (15), 3919–3923. https://doi.org/10.1002/grl.50767.
Quinn, B., Murphy, F., Ewins, C., 2017. Validation of density separation for the rapid recovery of microplastics from sediment. Anal. Methods 9, 1491–1498. https://doi.org/10.1039/C6AY02542K.
Rakib, Md.R.J., Hossain, M.B., Kumar, R., Ullah, Md.A., Al Nahian, S., Rima, N.N., Choudhury, T.R., Liba, S.I., Yu, J., Khandaker, M.U., Sulieman, A., Sayed, M.M., 2022. Spatial distribution and risk assessments due to the microplastics pollution in sediments of Karnaphuli River Estuary, Bangladesh. Sci. Rep. 12, 8581. https://doi.org/10.1038/s41598-022-12296-0.
Rech, S., Macaya-Caquilpán, V., Pantoja, J.F., Rivadeneira, M.M., Jofre Madariaga, D., Thiel, M., 2014. Rivers as a source of marine litter – a study from the SE Pacific. Mar. Pollut. Bull. 82, 66–75. https://doi.org/10.1016/j.marpolbul.2014.03.019.
Remy, F., Collard, F., Gilbert, B., Compère, P., Eppe, G., Lepoint, G., 2015. When microplastic is not plastic: the ingestion of artificial cellulose fibers by macrofauna living in seagrass Macrophytodetritus. Environ. Sci. Technol. 49, 11158–11166. https://doi.org/10.1021/acs.est.5b02005.
Rochman, C.M., Tahir, A., Williams, S.L., Baxa, D.V., Lam, R., Miller, J.T., Teh, F.-C., Werorilangi, S., Teh, S.J., 2015. Anthropogenic debris in seafood: plastic debris and fibers from textiles in fish and bivalves sold for human consumption. Sci. Rep. 5, 14340. https://doi.org/10.1038/srep14340.
Saliu, F., Montano, S., Lasagni, M., Galli, P., 2020. Biocompatible solid-phase microextraction coupled to liquid chromatography triple quadrupole mass spectrometry analysis for the determination of phthalates in marine invertebrate. J. Chromatogr. A 1618, 460852. https://doi.org/10.1016/j.chroma.2020.460852.
Saliu, F., Veronelli, M., Raguso, C., Barana, D., Galli, P., Lasagni, M., 2021. The release process of microfibers: from surgical face masks into the marine environment. Environ. Adv. 4, 100042. https://doi.org/10.1016/j.envadv.2021.100042.
Saliu, F., Lasagni, M., Andò, S., Ferrero, L., Pellegrini, C., Calafat, A., Sanchez-Vidal, A., 2022. A baseline assessment of the relationship between microplastics and plasticizers in sediment samples collected from the Barcelona continental shelf. ESPR 1-14. https://doi.org/10.1007/s11356-022-24772-1.
Sanchez-Vidal, A., Thompson, R.C., Canals, M., De Haan, W.P., 2018. The imprint of microfibres in southern European deep seas. PLoS One 13 (11), e0207033. https://doi.org/10.1371/journal.pone.0207033.
Scherer, C., Weber, A., Stock, F., Vurusic, S., Egerci, H., Kochleus, C., Arendt, N., Foeldi, C., Dierkes, G., Wagner, M., Brennholt, N., Reifferscheid, G., 2020. Comparative assessment of microplastics in water and sediment of a large European river. Sci. Total Environ. 738, 139866. https://doi.org/10.1016/j.scitotenv.2020.139866.

Schieber, J., 2011. Reverse engineering mother nature—shale sedimentology from an experimental perspective. Sediment. Geol. 238 (1–2), 1–22.
Schmidt, C., Krauth, T., Wagner, S., 2017. Export of plastic debris by Rivers into the sea. Environ. Sci. Technol. 51, 12246–12253. https://doi.org/10.1021/acs.est.7b02368.
Shabaka, S., Moawad, M.N., Ibrahim, M.I.A., El-Sayed, A.A.M., Ghobashy, M.M., Hamouda, A.Z., El-Alfy, M.A., Darwish, D.H., Youssef, N.A.E., 2022. Prevalence and risk assessment of microplastics in the Nile Delta estuaries: "The Plastic Nile" revisited. Sci. Total Environ. 852, 158446. https://doi.org/10.1016/j.scitotenv.2022.158446.
Sherwood, C., Book, J., Carniel, S., Cavaleri, L., Chiggiato, J., Das, H., Doyle, J., Harris, C., Niedoroda, A., Perkins, H., Poulain, P.-M., Pullen, J., Reed, C., Russo, A., Sciavo, M., Signell, R., Trykovski, P., Warner, J., 2004. Sediment dynamics in the Adriatic Sea investigated with coupled models. Oceanography 17, 58–69. https://doi.org/10.5670/oceanog.2004.04.
Shruti, V.C., Kutralam-Muniasamy, G., 2023. Blanks and bias in microplastic research: implications for future quality assurance. Trends Environ. Anal. Chem. 38, 1–9 e00203.
Simon-Sánchez, L., Grelaud, M., Garcia-Orellana, J., Ziveri, P., 2019. River deltas as hotspots of microplastic accumulation: the case study of the Ebro River (NW Mediterranean). Sci. Total Environ. 687, 1186–1196. https://doi.org/10.1016/j.scitotenv.2019.06.168.
Singh, N., Mondal, A., Bagri, A., Tiwari, E., Khandelwal, N., Monikh, F.A., Darbha, G.K., 2021. Characteristics and spatial distribution of microplastics in the lower Ganga River water and sediment. Mar. Pollut. Bull. 163, 111960. https://doi.org/10.1016/j.marpolbul.2020.111960.
Sruthy, S., Ramasamy, E.V., 2017. Microplastic pollution in Vembanad Lake, Kerala, India: the first report of microplastics in lake and estuarine sediments in India. Environ. Pollut. 222, 315–322. https://doi.org/10.1016/j.envpol.2016.12.038.
Stanton, T., Johnson, M., Nathanail, P., MacNaughtan, W., Gomes, R.L., 2019. Freshwater and airborne textile fibre populations are dominated by 'natural', not microplastic, fibres. Sci. Total Environ. 666, 377–389. https://doi.org/10.1016/j.scitotenv.2019.02.278.
Stevenson, C.J., Talling, P.J., Masson, D.G., Sumner, E.J., Frenz, M., Wynn, R.B., 2014. The spatial and temporal distribution of grain-size breaks in turbidites. Sedimentology 61 (4), 1120–1156. https://doi.org/10.1111/sed.12091.
Stile, N., Raguso, C., Pedruzzi, A., Cetojevic, E., Lasagni, M., Sanchez-Vidal, A., Saliu, F., 2021. Extraction of microplastic from marine sediments: a comparison between pressurized solvent extraction and density separation. Mar. Pollut. Bull. 168, 112436. https://doi.org/10.1016/j.marpolbul.2021.112436.
Suaria, G., Avio, C.G., Mineo, A., Lattin, G.L., Magaldi, M.G., Belmonte, G., Moore, C.J., Regoli, F., Aliani, S., 2016. The Mediterranean plastic soup: synthetic polymers in Mediterranean surface waters. Sci. Rep. 6, 37551. https://doi.org/10.1038/srep37551.
Suaria, G., Achtypi, A., Perold, V., Lee, J.R., Pierucci, A., Bornman, T.G., Aliani, S., Ryan, P.G., 2020. Microfibers in oceanic surface waters: a global characterization. Sci. Adv. 6, eaay8493. https://doi.org/10.1126/sciadv.aay8493.
Syvitski, J.P.M., Vörösmarty, C.J., Kettner, A.J., Green, P., 2005a. Impact of humans on the flux of terrestrial sediment to the global Coastal Ocean. Science 308, 376–380. https://doi.org/10.1126/science.1109454.
Syvitski, J.P.M., Kettner, A.J., Correggiari, A., Nelson, B.W., 2005b. Distributary channels and their impact on sediment dispersal. Mar. Geol. 222, 75–94. https://doi.org/10.1016/j.margeo.2005.06.030.
Syvitski, J.P.M., Kettner, A.J., Overeem, I., Hutton, E.W.H., Hannon, M.T., Brakenridge, G.R., Day, J., Vörösmarty, C., Saito, Y., Giosan, L., Nicholls, R.J., 2009. Sinking deltas due to human activities. Nat. Geosci. 2, 681–686. https://doi.org/10.1038/ngeo629.
Syvitski, J., Ángel, J.R., Saito, Y., Overeem, I., Vörösmarty, C.J., Wang, H., Olago, D., 2022. Earth's sediment cycle during the Anthropocene. Nat. Rev. Earth Environ. 3, 179–196. https://doi.org/10.1038/s43017-021-00253-w.
Ta, A.T., Babel, S., 2020. Microplastics pollution with heavy metals in the aquaculture zone of the Chao Phraya River Estuary, Thailand. Mar. Pollut. Bull. 161, 111747. https://doi.org/10.1016/j.marpolbul.2020.111747.
Talling, P.J., Masson, D.G., Sumner, E.J., Malgesini, G., 2012. Subaqueous sediment density flows: depositional processes and deposit types. Sedimentology 59, 1937–2003. https://doi.org/10.1111/j.1365-3091.2012.01353.x.
Taylor, M.L., Gwinnett, C., Robinson, L.F., Woodall, L.C., 2016. Plastic microfibre ingestion by deep-sea organisms. Sci. Rep. 6 (1), 1–9. https://doi.org/10.1038/srep33997.
Tesi, T., Miserocchi, S., Acri, F., Langone, L., Boldrin, A., Hatten, J.A., Albertazzi, S., 2013. Flood-driven transport of sediment, particulate organic matter, and nutrients from the Po River watershed to the Mediterranean Sea. J. Hydrol. 498, 144–152. https://doi.org/10.1016/j.jhydrol.2013.06.001.
Thompson, R.C., Moore, C.J., vom Saal, F.S., Swan, S.H., 2009a. Plastics, the environment and human health: current consensus and future trends. Philos. Trans. R. Soc. B Biol. Sci. 364, 2153–2166. https://doi.org/10.1098/rstb.2009.0053.
Thompson, R.C., Swan, S.H., Moore, C.J., vom Saal, F.S., 2009b. Our plastic age. Philos. Trans. R. Soc. B Biol. Sci. 364, 1973–1976. https://doi.org/10.1098/rstb.2009.0054.
Traykovski, P., Wiberg, P.L., Geyer, W.R., 2007. Observations and modeling of wave-supported sediment gravity flows on the Po prodelta and comparison to prior observations from the eel shelf. Cont. Shelf Res. 27, 375–399. https://doi.org/10.1016/j.csr.2005.07.008.
Trincardi, F., Amorosi, A., Bosman, A., Correggiari, A., Madricardo, F., Pellegrini, C., 2020. Ephemeral rollover points and clinothem evolution in the modern Po Delta based on repeated bathymetric surveys. Basin Res. 32, 402–418. https://doi.org/10.1111/bre.12426.
Trincardi, F., Francocci, F., Pellegrini, C., Ribera d'Alcalà, M., Sprovieri, M., 2023. The Mediterranean Sea in the Anthropocene. Oceanography of the Mediterranean Sea. Elsevier, pp. 501–553 https://doi.org/10.1016/B978-0-12-823692-5.00013-3.
Tunis, G., Uchman, A., 1996. Trace fossils and facies changes in cretaceous-Eocene flysch deposits of the Julian Prealps (Italy and Slovenia): consequences of regional and world-wide changes. Ichnos 4, 169–190. https://doi.org/10.1080/10420949609380125.
Uchman, A., 2004. Phanerozoic history of deep-sea trace fossils. Geol. Soc. Lond. Spec. Publ. 228, 125–139. https://doi.org/10.1144/GSL.SP.2004.228.01.07.
Umgiesser, G., Ferrarin, C., Cucco, A., De Pascalis, F., Bellafiore, D., Ghezzo, M., Bajo, M., 2014. Comparative hydrodynamics of 10 Mediterranean lagoons by means of numerical modeling. J. Geophys. Res. Oceans 119 (4), 2212–2226.
UNEP, 2016. UNEP Frontiers 2016 Report: Emerging Issues of Environmental Concern. United Nations Environment Programme, NairobiUnited Nations Environment Programme.
Van der Wal, M., van der Meulen, M., Tweehuijsen, G., Peterlin, M., Palatinus, A., Kovac Viršek, M., 2015. SFRA0025: Identification and Assessment of Riverine Input of (Marine) Litter. Report for Michail Papadoyannakis. DG Environment, United Kingdom, p. 186.
Vianello, A., Boldrin, A., Guerriero, P., Moschino, V., Rella, R., Sturaro, A., Da Ros, L., 2013. Microplastic particles in sediments of Lagoon of Venice, Italy: first observations on occurrence, spatial patterns and identification. Estuar. Coast. Shelf Sci. 130, 54–61. https://doi.org/10.1016/j.ecss.2013.03.022.
Waldschläger, K., Brückner, M.Z.M., Carney Almroth, B., Hackney, C.R., Adyel, T.M., Alimi, O.S., Belontz, S.L., Cowger, W., Doyle, D., Gray, A., Kane, I., Kooi, M., Kramer, M., Lechthaler, S., Michie, L., Nordam, T., Pohl, F., Russell, C., Thit, A., Umar, W., Valero, D., Varrani, A., Warrier, A.K., Woodall, L.C., Wu, N., 2022. Learning from natural sediments to tackle microplastics challenges: a multidisciplinary perspective. Earth-Sci. Rev. 228, 104021. https://doi.org/10.1016/j.earscirev.2022.104021.
Walling, D.E., Woodward, J.C., 1993. Use of a field-based water elutriation system for monitoringthe in situ particle size characteristics of fluvial suspended sediment. Water Res. 27 (9), 1413–1421.
Wang, X.H., Pinardi, N., 2002. Modeling the dynamics of sediment transport and resuspension in the northern Adriatic Sea. J. Geophys. Res. Oceans 107 (C12). https://doi.org/10.1029/2001JC001303 (18-1).
Weideman, E.A., Perold, V., Ryan, P.G., 2020. Limited long-distance transport of plastic pollution by the Orange-Vaal River system, South Africa. Sci. Total Environ. 727, 138653. https://doi.org/10.1016/j.scitotenv.2020.138653.
Weiss, L., Ludwig, W., Heussner, S., Canals, M., Ghiglione, J.-F., Estournel, C., Constant, M., Kerhervé, P., 2021. The missing ocean plastic sink: gone with the rivers. Science 373, 107–111. https://doi.org/10.1126/science.abe0290.
Wentworth, C.K., 1922. A scale of grade and class terms for clastic sediments. J. Geol. 30, 377–392. https://doi.org/10.1086/622910.
Wheatcroft, R.A., Stevens, A.W., Hunt, L.M., Milligan, T.G., 2006. The large-scale distribution and internal geometry of the fall 2000 Po River flood deposit: evidence from digital X-radiography. Cont. Shelf Res. 26, 499–516. https://doi.org/10.1016/j.csr.2006.01.002.
Willis, K.A., Eriksen, R., Wilcox, C., Hardesty, B.D., 2017. Microplastic distribution at different sediment depths in an urban estuary. Front. Mar. Sci. 4, 419. https://doi.org/10.3389/fmars.2017.00419.
Woodall, L.C., Sanchez-Vidal, A., Canals, M., Paterson, G.L.J., Coppock, R., Sleight, V., Calafat, A., Rogers, A.D., Narayanaswamy, B.E., Thompson, R.C., 2014. The deep sea is a major sink for microplastic debris. R. Soc. Open Sci. 1, 140317. https://doi.org/10.1098/rsos.140317.
Wright, S.L., Kelly, F.J., 2017. Plastic and human health: a micro issue? ES&T 51 (12), 6634–6647. https://doi.org/10.1021/acs.est.7b00423.
Wu, N., Zhang, Y., Zhang, X., Zhao, Z., He, J., Li, W., Ma, Y., Niu, Z., 2019. Occurrence and distribution of microplastics in the surface water and sediment of two typical estuaries in Bohai Bay, China. Environ Sci Process Impacts 21, 1143–1152. https://doi.org/10.1039/C9EM00148D.
Xiong, X., Wu, C., Elser, J.J., Mei, Z., Hao, Y., 2019. Occurrence and fate of microplastic debris in middle and lower reaches of the Yangtze River–from inland to the sea. Sci. Total Environ. 659, 66–73. https://doi.org/10.1016/j.scitotenv.2018.12.313.
Zavala, C., Arcuri, M., Blanco Valiente, L., 2012. The importance of plant remains as diagnostic criteria for the recognition of ancient hyperpycnites. Rev. Paléobiol. 11, 457–469.
Zhong, G., Peng, X., 2021. Transport and accumulation of plastic litter in submarine canyons—the role of gravity flows. Geology 49 (5), 581–586. https://doi.org/10.1130/G48536.1.